BMC Genomics

RESEARCH

Open Access

Transcriptomic and biometric parameters analysis in rainbow trout (Oncorhynchus mykiss) challenged with viral hemorrhagic septicemia virus (VHSV)

Mohammad Ghaderzadeh[1*], Ghodrat Rahimi-Mianji[1], Ardeshir Nejati-Javaremi[2] and Nastaran Shahbazian[3]

Abstract

Background Viral hemorrhagic septicemia virus (VHSV) is a highly pathogenic virus that poses a significant threat to the health of diverse marine species. Among these, trout species, particularly rainbow trout (*Oncorhynchus mykiss*), are highly susceptible. This study evaluated the effects of VHSV infection on the biometric traits of rainbow trout and investigated the molecular mechanisms associated with the disease.

Results Biometric traits of fish were collected and documented weekly during the fourth and fifth weeks of the experiment. A statistically significant difference in body weight was observed in the fifth week, particularly between the control group and the groups injected with either physiological saline or the virus. Additionally, body length-related attributes showed significant variation across all treatment groups within the designated timeframe. RNA was extracted from spleen tissue of the group injected with high doses of physiological saline and the group injected with high doses of the virus using the TRIzol protocol. Differential gene expression analysis revealed 1,726 genes with significant differences between the two groups. Several key immune-related genes were identified, including TLR2, TLR7, TLR8, TLR22, IRF5, IRF6, IRF7, IRF8, IRF10, IL11a, IL12B, IL1b, IL7R, ILR1 II, HSP90B1, HSP47, TNF-α, TRF3, SPRY1, CASP3, FN1, GAPDH, and IgGFc-binding proteins. Network-based analysis of differentially expressed genes was conducted using the GeneMANIA module in Cytoscape, and metabolic pathways were identified through the DAVID database. The results highlighted the involvement of key pathways, including the Toll-like receptor pathway, p53 signaling pathway, PPAR signaling pathway, and the cell cycle, in the infected group. Validation tests for selected upregulated (EPCAM, APOC2 and XDD4) and downregulated (TLR7, XDH, and TSPAN36) candidate genes, were conducted using qRT-PCR. The qPCR results showed a strong and statistically significant correlation with the RNA-seq data, confirming the reliability of the findings.

Conclusions VHSV significantly impacts the growth of rainbow trout, affecting both body length and gene expression. This study underscores the substantial economic risks posed by the virus and the absence of an effective cure, highlighting the importance of preventative measures. Additionally, potential resistance genes and pathways were identified through RNA sequencing, providing valuable insights for improving trout breeding programs.

Keywords Rainbow trout, RNA-seq, Gene network, Viral hemorrhagic septicemia virus

*Correspondence:
Mohammad Ghaderzadeh
mg.mahabad1365@gmail.com
Full list of author information is available at the end of the article

Background

The first isolation of Viral Hemorrhagic Septicemia Virus (VHSV) from European rainbow trout (*Oncorhynchus mykiss*) was reported by [1]. Since then, the virus has been identified in over 82 different fish species worldwide [2, 3]. Infectious diseases are widespread in marine ecosystems, causing devastating economic losses in the aquaculture industry and posing significant threats to fisheries [4, 5]. Viral infections account for 25% of common marine diseases and impact 49% of fish species. The high mortality rates of wild fish in large lakes due to viral diseases have drawn considerable attention from both researchers and governments to investigate the underlying causes and identify the infectious agents responsible [4].

Viral hemorrhagic septicemia (VHS) is classified as a major aquatic disease by the World Organization for Animal Health (OIE). Despite extensive efforts, no effective treatment exists to control its spread [6]. VHSV affects a wide range of marine species, with rainbow trout (*Oncorhynchus mykiss*) being particularly susceptible [7]. A member of the *Rhabdoviridae* family and *Novirhabdovirus* genus, VHSV possesses a negative-strand RNA genome approximately 12 kbp in length. This genome encodes five structural proteins: nucleoprotein (N), phosphoprotein (P), matrix protein (M), glycoprotein (G), and RNA polymerase (L) as well as a nonstructural protein (NV) [8, 9]. Numerous studies have investigated the molecular mechanisms and key genes associated with VHSV infection and resistance [5, 7, 10–14]. Research on rainbow trout (*Oncorhynchus mykiss*) has examined both resistant and susceptible lines, resulting in the identification and precise mapping of quantitative trait loci (QTL). These studies highlight the critical role of interferon and interferon-stimulated genes in enhancing the innate immunity of rainbow trout, thereby strengthening their defenses against VHSV. In particular, cell lines A22 and B57 infected with inactivated VHSV exhibited heightened resistance responses. Additionally, the identification of genes associated with innate immunity located near QTLs in the rainbow trout (*Oncorhynchus mykiss*) genome provides further evidence supporting these findings [5].

Wild strains of viral hemorrhagic septicemia virus (VHSV) are associated with higher mortality rates in farmed salmon (*Salmo salar*), whereas strains isolated from marine fish have shown reduced disease severity in rainbow trout (*Oncorhynchus mykiss*) [7]. Comprehensive genomic analyses of various marine and freshwater species suggest that a small number of amino acids may significantly influence the severity of VHSV infections in rainbow trout (*Oncorhynchus mykiss*) [7]. Recent studies have identified specific genetic markers within the NV and N proteins that are associated with virulence. These findings underscore the genetic diversity of VHSV and its potential impact on disease severity and outcomes in aquaculture species [1].

The advent of RNA-seq technology has significantly advanced transcriptional studies in various fish species, including zebrafish (*Danio rerio*), channel catfish (*Ictalurus punctatus*), European bass (*Dicentrarchus labrax*), and rainbow trout (*Oncorhynchus mykiss*) [13–15]. By analyzing fish transcripts before and after exposure to challenges, researchers can identify genes and pathways associated with immune responses. Furthermore, RNA-seq facilitates the identification and selection of disease-resistant fish and enables the examination of gene expression in different tissues under varying conditions [14].

The relationship between hosts and parasites or viruses is complex and warrants further investigation. Studying specific genes and mechanisms involved in disease resistance provides valuable insights for developing enhanced strategies to combat infections [16].

Fish resistance to pathogens, including viruses and bacteria, is influenced by genetic factors [17]. Analyzing the expression of immunity-related genes in response to pathogens provides valuable insights into identifying genes that confer resistance to aquatic diseases. Additionally, exploring immune genes within the context of vaccine development holds significant potential [18]. Immunological studies on rainbow trout (*Oncorhynchus mykiss*) are particularly important due to their critical role in food production and their direct contributions to agriculture and industry [19].

Evaluating biometric parameters in rainbow trout (*Oncorhynchus mykiss*) during VHSV infection provides critical insights into the impact of viral pathogens on fish physiology and health [20]. Biometric data, such as body weight, total length, fork length, and standard length, are essential in fisheries science as indicators of physiological status, health, immune responses, and disease resistance [21]. Body condition, a key marker of fish health, reflects energy allocation and overall physiological status [22, 23]. While morphometric indices are commonly used to assess body condition in relation to energy reserves, they also correlate with chronic stress, parasite load, and oxidative stress [24–26]. Monitoring these biometric metrics allows researchers to evaluate the severity of infections like VHSV and their effects on critical traits associated with immunity and disease resistance, thereby deepening the understanding of fish health [20]. Combining biometric evaluations with transcriptomic analyses provides a comprehensive perspective on VHSV, enabling more precise interventions and the discovery of novel genetic markers for selective breeding programs.

This integrated approach contributes to the development of disease-resistant trout strains, enhancing the sustainability and economic viability of aquaculture [20].

This study investigated the effects of VHSV on rainbow trout (*Oncorhynchus mykiss*), focusing on its economic impact and the critical role of genetic mechanisms in disease resistance. The primary objective was to evaluate fish biometric traits, including growth, standard length, fork length, and total length, during VHSV infection. Genome-wide expression profiling using high-throughput sequencing was conducted to track gene expression changes, coupled with pathway enrichment analysis to identify virus-affected pathways. The study aimed to pinpoint specific genes and signaling pathways altered by VHSV, providing potential targets for breeding programs to enhance disease resistance. By identifying interventions to mitigate the effects of VHSV on rainbow trout (*Oncorhynchus mykiss*) populations, this research supports the development of selective breeding strategies to improve disease resistance and ensure the sustainability of aquaculture practices.

Methods

Location and experimental design

This study was conducted at the Aquaculture Laboratory Technology Incubator Center, Islamic Azad University, Roudehen Branch, located in Roudehen county, Tehran Province, Iran. A total of 310 fish, each weighing between 86 and 97 g, were obtained from a VHSV-free industrial fish farm in Alashtar County, Lorestan Province, Iran, and subsequently transported to Roudehen, Tehran Province.

The fish were housed in 18 open rectangular fiberglass tanks, each with dimensions of 0.92 m in width, 0.96 m in length, and 1.2 m in depth, providing a volume of 1.058 m^3 per tank. The stocking density was maintained at 1.7 kg /m^3, with 17 fish held in 1,058 L of water, corresponding to a cultivation density of 1.5 kg/m^3 [20].

Fish maintenance

A total of 310 fish were housed in tanks and fed a commercial diet three times daily (Simia, Iran). The required amount of food was calculated based on the live weight of the fish, using the feeding guidelines provided on the food packaging. Meals were administered in the morning, noon, and evening. Tank cleaning and siphoning were performed twice daily. Before the start of the experiments, the fish underwent a two-week acclimation period [20]. The experiment utilized a closed water system with automatic flow every 3 h. The total duration of the study, including the acclimation period and the completion of tissue sampling, was one month [19, 20].

Physical and chemical quality of water conditions

The water used in this investigation was sourced from a pit and stored in a 5,000-L fiberglass tank for 8 h prior to use. During the farming period, key water quality parameters, including temperature, pH, salinity, dissolved oxygen, and ammonium levels, were measured weekly using the KARIZAB Kit (Karizab, Iran; http://www.karizab.com). The water conditions were maintained at consistent levels throughout the study: temperature at 10 °C, pH at 7.5, salinity at 3 ppt, and dissolved oxygen at 10.2 mg/L [20].

Virus preparation

The VHSV strain used in this study belongs to genotype Ia. It was cultured at the National Reference Laboratory for Applied Studies and Diagnosis, affiliated with the Veterinary Organization of Alborz Province in Karaj, Iran. The virus was prepared for the study following the methods described in references [27, 28].

Viral challenge

After transferring 310 fish to the research center and completing the acclimation period, 29 fish died, leaving 281 fish available for experimental treatments. The study included five randomly treatment groups, labeled A, B, C, D, and E, which were randomly assigned. Groups A and B were injected with 0.03 ml and 0.06 ml of VHSV, respectively, while groups C and D received 0.03 ml and 0.06 ml of physiological saline (PHSA). Group E, the control group, did not receive any injections. Each group consisted of 60 fish, except for group E, which included 41 fish [20].

Biometric traits analysis

Biometric measurements, including body weight and lengths (standard length, fork length, and final length), were recorded on days 28 and 35 of the rearing period. A one-way analysis of variance (ANOVA) was conducted to evaluate all biometric data. Tukey's Honestly Significant Difference (HSD) test was used to compare the means among the different experimental groups. All statistical analyses were performed using R software (version 1.6.3; https://www.r-project.org/).

Identification of VHSV and RNA preparation

To identify VHSV in the fish groups, spleen samples were collected and analyzed using RT-PCR [29]. Tissue samples were preserved with RNAlater® RNA Stabilization Reagent (Qiagen, Hilden, Germany). Subsequently, spleen tissues from two groups (one infected with 0.06 mL VHSV and the other administered 0.06 mL physiological saline) were selected for RNA extraction.

Total RNA was isolated using the TRIzol RNA isolation protocol (Invitrogen, Carlsbad, CA). The quality and integrity of the extracted RNA were assessed using a Nanodrop 2000 and an Agilent 2100 bioanalyzer before library construction. The primer sequences used for RT-PCR were as follows: VN For (5' ATG GAA GGA GGA ATT CGT GAA GCG 3') and VN Rev (5' GCG GTG AAG TGC TGC AGT TCC C 3'), which amplified a 505 bp fragment of the VHSV N-gene [29].

Library preparation and RNA-sequencing

During the RNA sequencing procedure, samples with the highest RNA quality and an RNA Integrity Number (RIN > 7.0) were selected for each replicate. Each RNA sample was derived from pooled spleen tissue collected from ten fish. mRNA-seq libraries were generated using Poly-A RNA and the TruSeq™ RNA Sample Preparation Kit (Illumina), following the manufacturer's protocols. A total of six libraries were prepared, comprising three samples each from the PHSA-treated and VHSV-treated groups. Paired-end sequencing with a read length of 150 bp was performed on a HiSeq2500 platform (Illumina) at Novogene Company, Beijing, China.

RNA sequencing data analysis

Before analysis, raw Illumina HiSeq-2500 data were subjected to quality control using FastQC [30]. Quality metrics were assessed based on a nucleotide quality threshold of $Q \geq 30$. Low-quality read pairs and residual adapters were removed using Trimmomatic [31]. ensuring that only high-quality reads were retained for downstream analysis. Cleaned reads from each RNA-seq sample were first aligned using the spliced read aligner TopHat v2.0.11 [32] and Subsequently, Bowtie2 version 2.2.3 was used to further align the cleaned reads [33]. The alignment was performed against the rainbow trout (*Oncorhynchus mykiss*) reference genome (GenBank assembly accession number GCA_002163495.1) [34].

Differential gene expression analysis between samples treated with 0.06 mL VHSV and 0.06 mL PHSA was conducted using Cufflinks v2.2.1 [35]. The assembled transcripts generated by Cufflinks were combined into a unified transcriptome set using Cuffmerge v2.2.1 [35]. Differentially expressed transcripts were identified using the Cuffdiff utility v2.2.1 [35], applying a threshold of |Fold Change (FC)| > 1 to determine significant differences between the two groups.

To control the false discovery rate (FDR), multiple test corrections were applied using the Benjamini and Hochberg method, with a significance level set at $p < 0.05$. The visualization of Cuffdiff RNA-seq results was performed using the cummerbund R package (version 2.32.0) [36].

Biological pathways analysis

To understand the biological processes underlying changes in gene expression and the interactions among these genes, the KEGG database (Kyoto Encyclopedia of Genes and Genomes) was utilized as a resource for gene and genome information, (https://www.genome.jp/kegg/) [37]. Additionally, the online Database for Annotation, Visualization, and Integrated Discovery (DAVID) was used for further analyses (https://david.ncifcrf.gov/home.jsp). The GeneMANIA prediction server was employed, leveraging zebrafish (*Danio rerio*) data, to predict gene–gene networks, particularly for significant genes [38, 39].

Validation of differentially expressed transcripts by quantitative real-time PCR (qRT-PCR)

To validate the accuracy of RNA-seq differential expression, RNA samples from spleen tissue used for sequencing were also analyzed using qRT-PCR. The expression levels of six randomly selected genes, three upregulated (*ddx4*, *apoc2* and *epcam*) and three downregulated (*tspan36*, *xdh*, and *tlr7*) were measured using qRT-PCR with primers designed using Oligo v7 software [40]. As described in [41], cDNA synthesis was performed by mixing 4 µL of RNA with reverse transcriptase reagents and random hexamers (Promega) in a total volume of 25 µL. The qRT-PCR reactions, executed using a Bio-Rad thermocycler (Bio-Rad Laboratories Inc., Hercules, CA, USA) and SYBR Green Master Mix (Thermo Fisher Scientific, USA), followed the manufacturer's guidelines. The thermal cycling conditions consisted of: initial denaturation at 95 °C for 10 min, 40 cycles at 95 °C for 15 s, 60 °C for 30 s, 72 °C for 30 s, and a final extension at 72 °C for 5 min. Relative gene expression was measured using the Pfaffl method [42] with normalization to *β-actin* gene. The fold expression values were calculated by dividing the normalized expression of the experimental samples by the control values. The reactions for each gene were repeated three times, and a no-template control was used for each gene.

$$Expression\ ratio = \frac{\left(E_{target}\right)^{\triangle CP_{target(control-treatment)}}}{\left(E_{\beta\_actin}\right)^{\triangle CP_{\beta\_actin(control-treatment)}}}$$

primer efficiency for each gene was evaluated through a standard curve approach to ensure reliable quantification, as recommended by following formula: $E = 10^{-1/slope)}$ [43]. Differential expression between samples was analyzed using a Student's t-test, with a *p*-value of less than 0.05 considered statistically significant.

Results

Diagnosis of VHSV in the treated fish samples

To confirm VHSV infection in fish specimens, spleen tissue samples were analyzed. The RT-PCR protocol produced successful results consistent with established methodologies, and the amplified products were visualized via electrophoresis on a 1% agarose gel (Fig. 1).

As shown in Fig. 1, the targeted fragment of the VHSV N gene was successfully amplified. To ensure robust data validation, PCR analysis included samples from the virus-injected, non-injected, and physiological saline-injected groups. This comprehensive approach enabled a thorough assessment of potential contamination across all experimental groups.

The clear amplification of this gene fragment confirmed the unequivocal presence of the virus in the tested samples. Additionally, no viral gene amplification was observed in either the physiological saline-injected group or the control group.

RNA was extracted from six rainbow trout (*Oncorhynchus mykiss*) spleen samples using TRIzol reagent (Invitrogen, Carlsbad, CA, USA). The quality of the extracted RNA was assessed using an Agilent Bioanalyzer 2100 system. Only samples with an RNA Integrity Number (RIN) greater than 7 were selected for cDNA library construction [44].

The results of the RNA concentration determination and RIN assessment for the samples submitted to Novagen, China, are summarized in Table 1. (Table 1; Supplementary Tables section).

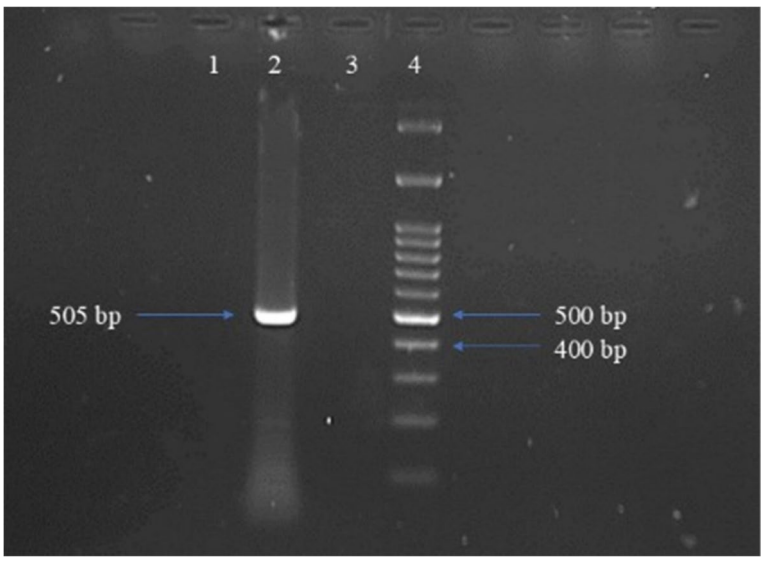

Fig. 1 A fragment of the N gene from VHSV with a length of 505 bp amplified by PCR. Lane 1: Control sample without injection, Lane 2: Sample with virus injection: 505 bp fragment associated with the N-gene region of the VHSV virus. Lane3: Sample with physiological saline injection, and Lane 4: 100 bp molecular weight marker (Tekaposist Company, Iran)

Table 1 RNA integrity (quality) index of sequenced samples

Sample Name	RNA (ng/ul)	Vol (ul)	OD260:280	OD260:230	RIN	Test Conclusion
PHSA_1	320	20	1.70	1.55	8.1	Pass
PHSA_2	240	20	2.35	0.81	8.3	Pass
PHSA_3	507	20	2.05	2.16	8.2	Pass
VHSV_1	610	20	1.94	2.24	7.8	Pass
VHSV_2	280	20	1.86	0.57	7.8	Pass
VHSV_3	334	20	2.01	1.59	7.5	Pass

Statistical analysis of biometric data

Thirty fish were randomly assigned to each treatment group. Analysis of weight data during the first week showed average weights of 105.75 g, 104.89 g, 107.19 g, 107.08 g, and 108.47 g for groups A, B, C, D, and E, respectively. The weight ranges recorded at the end of the first week for each group were as follows: 96.49–112.54 g (group A), 97.50–110.49 g (group B), 98.74–112.89 g (group C), 99.97–112.61 g (group D), and 101.75–114.39 g (group E) (Table 2; Supplementary Tables section).

As shown in Table 2, during the second week of the challenge, group E exhibited the highest average weight gain (114.65 g), while group A recorded the lowest weight gain (109.81 g). In group E, the maximum and minimum weights at the end of the second week were 119.8 g and 108.13 g, respectively. Similarly, in group A, the maximum and minimum weights were 115.24 g and 102.41 g, respectively.

Over the two-week challenge period, data on body weight characteristics (Table 2) revealed that the highest weight gain occurred in group E (control group), whereas the lowest weight gain was observed in groups B and A (virus-injected groups) (Table 2; Supplementary Tables section).

The total length (TL) of the fish is presented in Table 3 (Supplementary Tables section). During the first week of the challenge, the maximum total body length recorded was 20.46 cm (group E), while the minimum was 20.18 cm (group A). In group E, the maximum and minimum total body lengths recorded during the first week were 21.6 cm and 19.5 cm, respectively. Similarly, in group A, the maximum and minimum total body lengths were 21 cm and 19.4 cm, respectively (Table 3; Supplementary Tables section).

The total body length of the fish during the second week of the challenge was measured, recorded, and analyzed. As shown in Table 3, the highest average total body length (20.95 cm) was observed in group E, while the lowest average value (20.26 cm) was recorded in group A. For group E, the maximum and minimum total body lengths recorded during the second week were 22.2 cm and 19.6 cm, respectively. Similarly, in group A, the maximum and minimum total body

Table 2 Summary of biometric results for fish body weight during the first and second weeks of the virus challenge

Parameter (g)	Mean ± Standard deviation	Minimum values	Maximum values	Coefficient of Variation (%CV)
Weight of the first week of group A	105.75 ± 3.75	96.49	112.54	3.54
Weight of the first week of group B	104.89 ± 3.06	97.50	110.49	2.91
Weight of the first week of group C	107.19 ± 2.92	98.74	112.89	2.85
Weight of the first week of group D	107.08 ± 2.92	99.97	112.61	2.72
Weight of the first week of group E	108.47 ± 2.29	101.75	114.39	2.75
Weight of the second week of group A	109.81 ± 2.90	102.41	115.24	2.64
Weight of the second week of group B	109.92 ± 3.00	101.79	115.42	2.79
Weight of the second week of group C	113.21 ± 3.18	106.95	118.98	2.80
Weight of the second week of group D	113.57 ± 3.75	106.70	118.70	2.84
Weight of the second week of group E	114.65 ± 3.09	108.13	119.80	2.69

Table 3 Summary of biometric results of total fish length in the first and the second week of injection challenge

Parameter (cm)	Mean ± Standard deviation	Minimum values	Maximum values	Coefficient of variation (%CV)
TL in the first week in group E	20.46 ± 0.57	19.5	21.6	2.78
TL in the first week in group D	20.36 ± 0.8	19.4	21.2	3.92
TL in the first week in group C	20.39 ± 0.49	19.5	21.3	2.40
TL in the first week of group B	20.24 ± 0.55	19.3	21.1	2.71
TL in the first week in group A	20.18 ± 0.48	19.4	21	2.37
TL in the second week in group E	20.95 ± 0.77	19.6	22.2	3.67
TL in the second week in group D	20.79 ± 0.79	19.4	22	3.79
TL in the second week in group C	20.76 ± 0.80	19.5	22	3.85
TL in the second week in group B	20.34 ± 0.74	18.4	21.4	3.63
TL in the second week in group A	20.26 ± 0.64	19	21.5	3.15

lengths recorded were 21.5 cm and 19 cm, respectively (Table 3; Supplementary Tables section).

As shown in Table 3 (Supplementary Tables section), the recorded total body length values indicate that the fish in the non-injected group E had the highest total body length, while the fish in the virus-injected treatment group A exhibited the lowest total body length.

Biometric analysis of fish body weight at the end of the first week of the challenge revealed a statistically significant difference between groups E and A. Additionally, significant differences in body weight were observed between groups E and B ($P<0.05$). However, when comparing the average measurements across the five treatment groups, no significant differences were found in the biometric traits of standard length, fork length, or total body length during the first week of the challenge (Table 3; Supplementary Tables section).

At the end of the second week, analysis of average body weight indicated a highly significant difference ($P<0.001$) between groups E and A, as well as between groups D and A, C and A, and C and B, as shown in Table 4. Furthermore, during the second week of the challenge, a highly significant difference ($P<0.001$) in standard and fork length was observed between group E and all other treatment groups (A, D, C, and B). Analysis of total body length revealed a statistically significant difference ($P<0.05$) by the end of week two, with group E differing significantly from groups A and B only.

In summary, comparisons among the viral, control, and physiological saline groups revealed a significant difference in body weight only at the end of the first week. Analysis of body dimensions showed no significant effect on body length; however, body weight differences were significant during the second week. These findings suggest that the disease has a substantial impact on regulating body weight and longitudinal growth in fish.

RNA sequencing analysis

To elucidate the molecular mechanisms underlying the response to virus injection, cDNA libraries were generated from six spleen tissue samples of rainbow trout (*Oncorhynchus mykiss*), with three replicates from each treatment group: virus-injected (0.06 mL VHSV) and physiological saline-injected (0.06 mL PHSA).

A total of 68.5 million and 69.3 million raw paired-end reads were obtained from the PHSA and VHSV groups, respectively. After processing with Bowtie2 v2.2.3, an average of 80% of the clean reads uniquely aligned to the fish genome [34]. Comprehensive details of the raw and clean reads, along with the mapping results, are provided in Table 5.

Identification of differentially expressed genes

In this study, the Cummerbund package, integrated within the R software environment, was used to visualize gene expression results generated by the Cuffdiff

Table 4 Investigating biometric indicators of rainbow trout injected with VHSV and physiological saline (Mean ± Standard deviation)

	Parameter	Group E ($n=30$)	Group D ($n=30$)	Group C ($n=30$)	Group B ($n=30$)	Group A ($n=30$)
The first week of the challenge	Final weight (g)	108.47 ± 2.99^{a}	107.08 ± 2.92^{abc}	107.19 ± 3.06^{ab}	104.89 ± 3.06^{c}	105.75 ± 3.75^{bc}
	Standard length (cm)	18.35 ± 0.35^{a}	18.34 ± 0.25^{a}	18.38 ± 0.27^{a}	18.28 ± 0.27^{a}	18.27 ± 0.31^{a}
	Fork length (cm)	19.05 ± 0.38^{a}	18.93 ± 0.38^{a}	18.97 ± 0.32^{a}	18.90 ± 0.32^{a}	18.92 ± 0.32^{a}
	Final length (cm)	20.46 ± 0.57^{a}	20.36 ± 0.8^{a}	20.39 ± 0.49^{a}	20.24 ± 0.55^{a}	20.18 ± 0.48^{a}
The second week of the challenge	Final weight (g)	114.65 ± 3.09^{a}	113.57 ± 3.23^{a}	113.21 ± 3.18^{a}	109.92 ± 3.00^{b}	109.81 ± 2.90^{b}
	Standard length (cm)	19.07 ± 0.49^{a}	18.90 ± 0.51^{a}	18.83 ± 0.54^{a}	18.29 ± 0.45^{b}	18.28 ± 0.43^{b}
	Fork length (cm)	19.68 ± 0.60^{a}	19.54 ± 0.61^{a}	19.49 ± 0.65^{a}	18.73 ± 0.45^{b}	18.94 ± 0.51^{b}
	Final length (cm)	20.95 ± 0.77^{a}	20.79 ± 0.79^{ab}	20.76 ± 0.80^{ab}	20.34 ± 0.74^{b}	20.26 ± 0.64^{b}

Statistically similar results ($p \geq 0.05$) are indicated by groups sharing the same letters

Table 5 Summary of reads statistics for RNA-seq data

Sample name	Raw reads	Trimmed reads	Concordantly mapped reads	Discordantly mapped reads	Uniquely mapped reads (%)	Total mapping
PHSA_1	20,169,854	20,169,565	16,058,247	1,965,346	16,446,095(0.82)	18,050,593 (0.90)
PHSA_2	21,187,201	21,187,114	16,814,236	2,155,228	17,602,113(0.79)	18,969,464 (0.90)
PHSA_3	27,228,143	27,228,008	21,212,395	2,989,032	21,726,281(0.79)	24,201,427 (0.88)
VHSV_1	22,067,762	22,067,569	17,458,809	2,371,420	17,602,113(0.79)	19,830,229 (0.89)
VHSV_2	24,499,364	24,499,180	19,085,082	3,273,667	20,147,444(0.82)	22,358,749 (0.91)
VHSV_3	22,751,014	22,750,494	17,790,213	2,938,462	18,68,586(0.82)	20,728,675 (0.91)

package. This package enables the creation of high-quality graphics in various formats [36]. The Cuffdiff analysis included three biological replicates from the two treatment groups, VHSV and PHSA. A total of 52,824 genes were identified across both experimental groups, of which 1,726 were differentially expressed. Furthermore, the analysis revealed 93,133 gene isoforms, highlighting transcriptional diversity. Additionally, 60,885 transcription start sites (TSS) were identified, providing insights into transcription initiation. The study also identified 63,264 coding sequences (CDS), representing protein-coding regions.

This analysis also identified 52,824 promoter regions, shedding light on the critical regulatory elements involved in gene transcription. Additionally, 60,885 splicing events were documented, highlighting the widespread occurrence of alternative splicing mechanisms that contribute to mRNA diversity. Lastly, 42,353 regulatory genes, referred to as "relCDS" genes, were identified. These genes play pivotal roles in regulating gene expression and, consequently, various cellular processes.

These comprehensive findings provide a multifaceted view of the genomic landscape under the experimental conditions, paving the way for further in-depth exploration and interpretation of the molecular mechanisms underlying the observed differences in gene expression.

Figure 2 presents a key aspect of the analysis, the "count vs. dispersion" plot. This visual tool is essential for evaluating the relationship between count data and dispersion across genes under different experimental conditions, specifically the VHSV-injected and PHSA-injected groups. The plot illustrates the variability (dispersion) of data points relative to their mean count values across these conditions. Its primary purpose is to identify genes with pronounced dispersion, highlighting potential candidates for detailed examination in subsequent phases of analysis (Fig. 2).

Figure 3 (Left) illustrates the distribution of expression values for a specific gene under two experimental conditions: VHSV and PHSA injections. Figure 3 (Right) presents the same comparison, incorporating data from all replicates in both groups. The X-axis represents gene expression levels measured as fragments per kilobase of transcript per million mapped reads (FPKM), while the Y-axis indicates the density or frequency of observations across different gene expression levels.

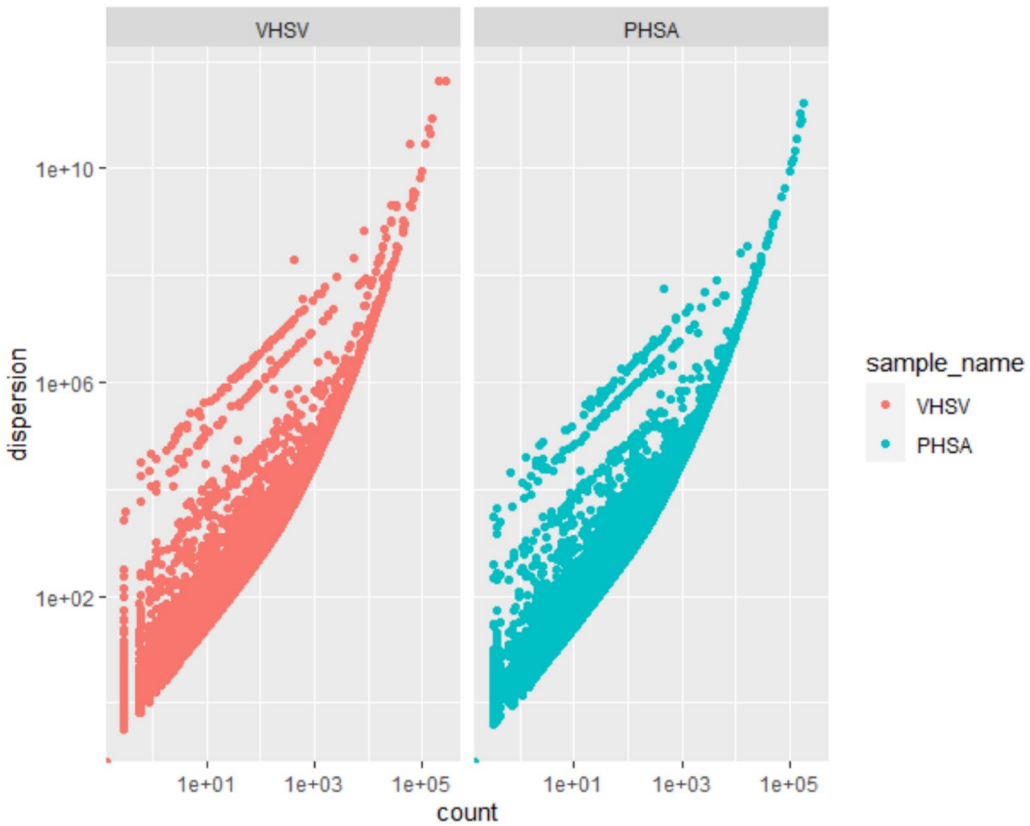

Fig. 2 The counts vs. dispersion plot in each VHSV and PHSA experimental groups

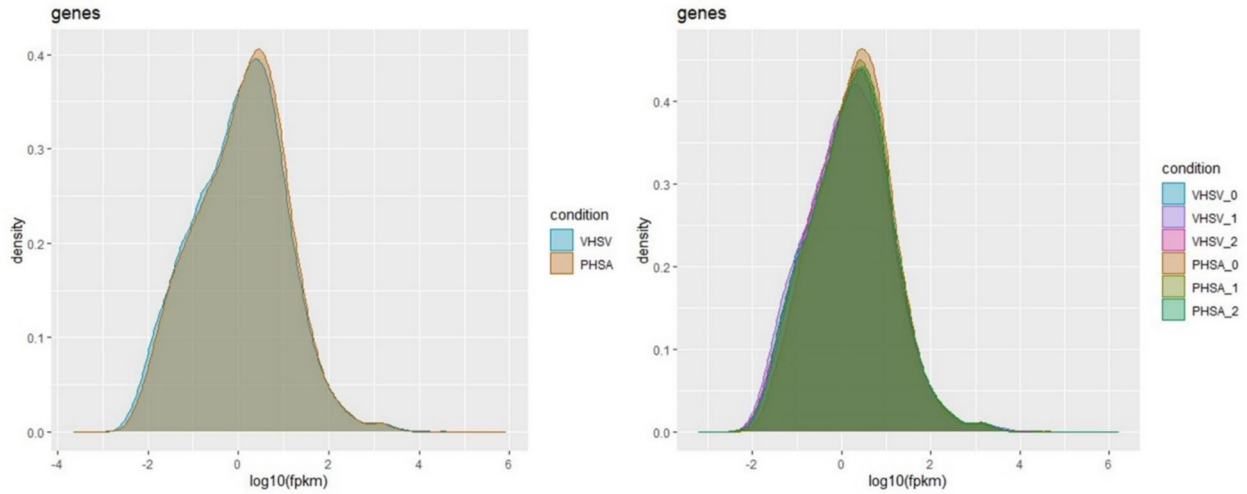

Fig. 3 (Left): Density plot of the individual VHSV vs. PHSA. (Right): Density plot comparing gene expression across biological replicates within the VHSV- and PHSA-treated groups

In the volcano plot representing gene expression in the two experimental groups (VHSV and PHSA), red points indicate genes with differential expression, while black points represent genes with similar expression levels in both groups. In this visualization, genes farther from the center of the plot exhibit greater variability in expression (Fig. 4). A significant difference in gene expression is observed when the -$\log_{10}$(p-value) exceeds 2, indicating that genes with p-values below 0.01 are statistically significant. These genes appear above the threshold of 2 on the y-axis in the volcano plot. On the right side of the plot, the red area highlights genes with high regulatory

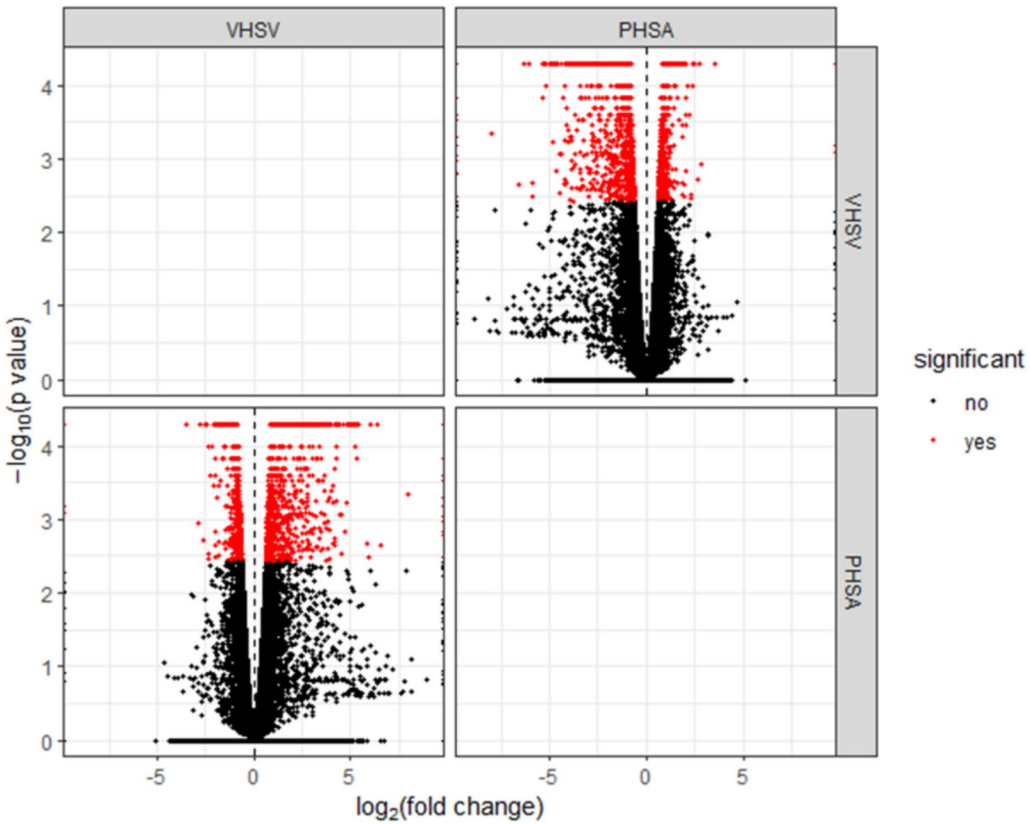

Fig. 4 Volcanic diagram of the expressed genes in the VHSV and PHSA experimental groups

limits, while on the left side, the red area identifies genes with low regulatory limits (Fig. 4).

The heatmap representation shows the VHSV group in purple and the PHSA group in orange, each consisting of three biological replicates, highlighting the differential gene expression observed in this study. The blue coloration indicates that all genes in the heatmap exhibit differential expression. A total of 1,726 differentially expressed genes were identified, of which 20 were randomly selected, normalized using the Z-score index, and clustered for further analysis. Genes displayed in green, with a positive Z-score, represent higher expression levels compared to the average, indicating elevated gene activity in those samples. Conversely, genes shown in red, with a negative Z-score, represent lower expression levels, reflecting reduced gene activity. This distribution underscores the intricate balance of gene expression levels within the samples (Fig. 5).

Principal Component Analysis (PCA) of RNA-seq data successfully revealed gene expression patterns associated with the VHSV and PHSA groups, including their biological replicates. These findings contribute to a better understanding of rainbow trout (*Oncorhynchus mykiss*) biology and provide valuable insights for

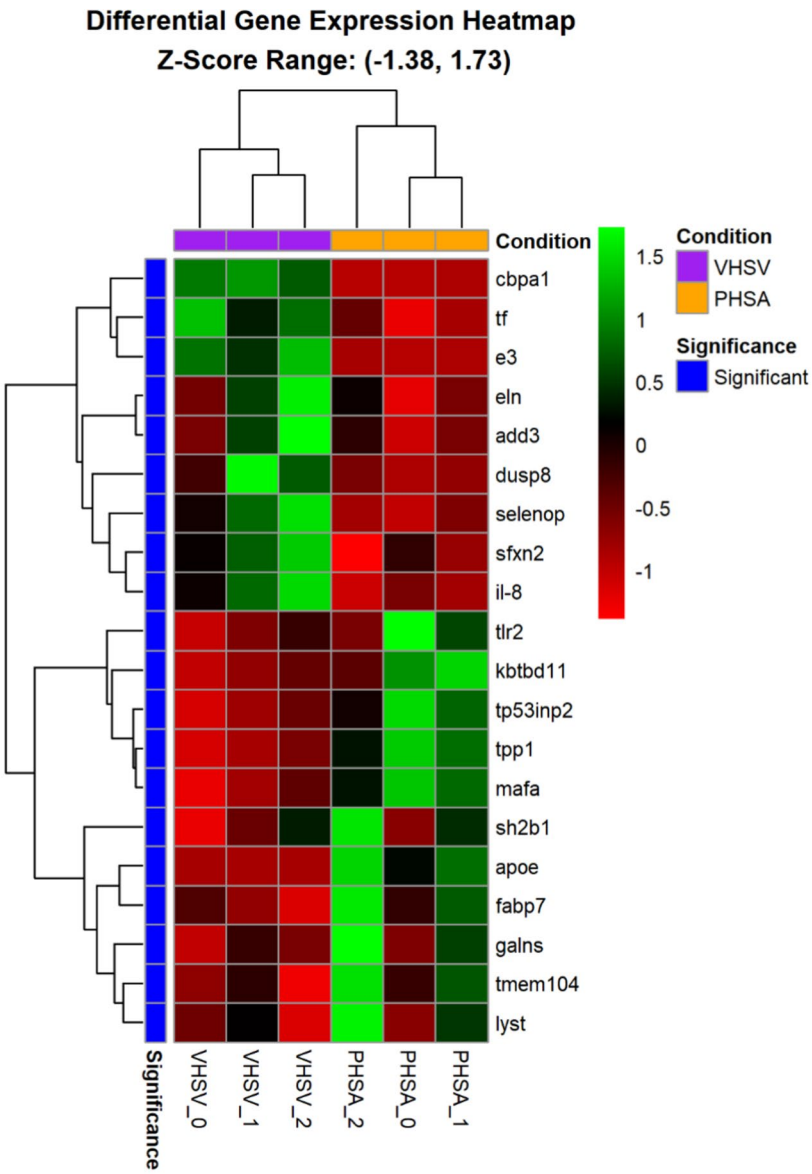

Fig. 5 Heatmap of differential gene expression between VHSV and PHSA conditions

future research and conservation programs. In Fig. 6, the treatment groups are clearly separated, with distinct gene expression patterns indicating complete differentiation within the treatment subgroups (including replicates). The primary objective of this analysis was to assess the similarity or difference between the gene expression profiles of the two experimental groups and to determine whether samples from the same treatment clustered together. The results demonstrated that all samples grouped into six distinct clusters corresponding to their treatments, based on the first two principal components. These transcriptomic changes may help identify candidate genes responsible for the observed differences between treatments (Fig. 6).

Functional enrichment analysis

The genes exhibiting differential expression in the VHSV and PHSA groups were further analyzed as upregulated and downregulated genes to investigate their functional roles in the viral response. This analysis identified 620 upregulated genes significantly associated with 12 KEGG pathways and 37 biological processes. In contrast, 1,045 downregulated genes were identified, revealing a significant association with 28 KEGG pathways and 193 biological processes (Supplementary File). Figure 7 highlights the key enriched biological process (BP) terms and KEGG pathways identified through this analysis.

The comparison between the virus-injected and physiological serum-injected groups identified several significant biological processes, as illustrated in Fig. 7. These

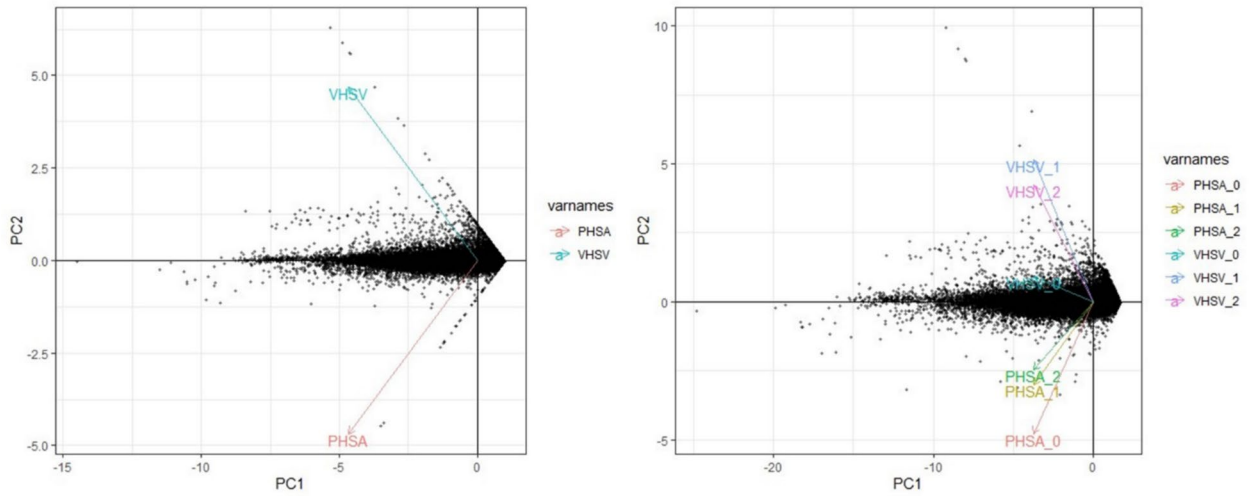

Fig. 6 PCA plots gene expression in two VHSV and PHSA groups

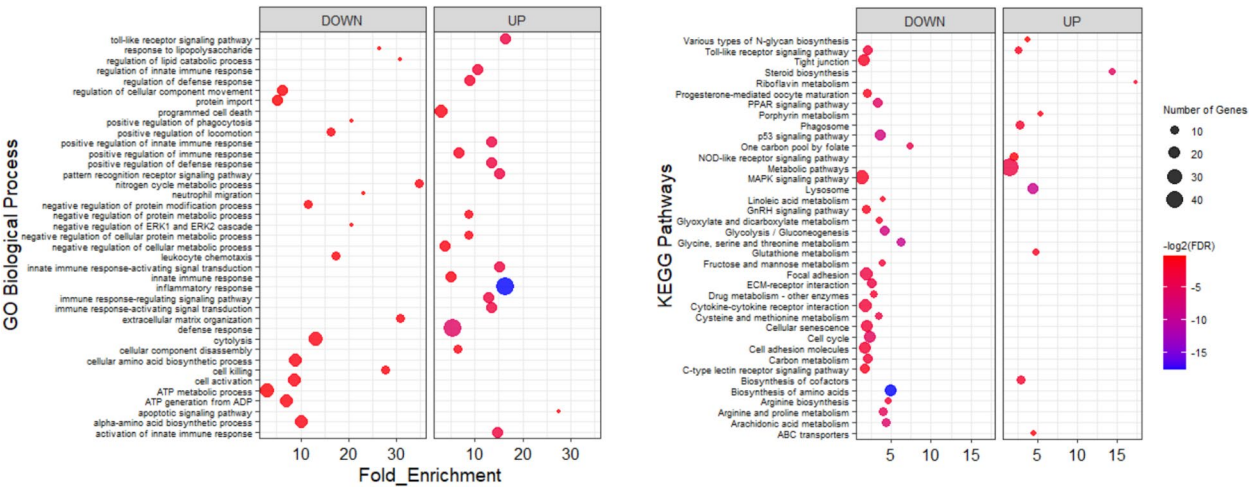

Fig. 7 Comparison analysis of up-and downregulated DEGs in the VHSV and PHSA experimental groups using GO and KEGG pathways

processes include the nitrogen cycle metabolic process, extracellular matrix organization, regulation of lipid catabolic process, cell killing, apoptotic signaling pathway, response to lipopolysaccharide, neutrophil migration, positive regulation of phagocytosis, negative regulation of the ERK1 and ERK2 cascade, leukocyte chemotaxis, inflammatory response, positive regulation of locomotion, Toll-like receptor signaling pathway, pattern recognition receptor signaling pathway, innate immune response-activating signal transduction, activation of innate immune response, positive regulation of defense response, immune response-activating signal transduction, positive regulation of innate immune response, cytolysis, immune response-regulating signaling pathway, negative regulation of protein modification process, regulation of innate immune response, alpha-amino acid biosynthetic process, regulation of defense response, cellular amino acid biosynthetic process, negative regulation of protein metabolic processes, cell activation, ATP generation from ADP, positive regulation of immune response, cellular component disassembly, regulation of cellular component movement, defense response, protein import, innate immune response, negative regulation of cellular metabolic processes, ATP metabolic process, and programmed cell death. Additionally, several significantly enriched pathways were identified, including amino acid biosynthesis; glycine, serine, and threonine metabolism; the p53 signaling pathway; glycolysis/gluconeogenesis; arachidonic acid metabolism; PPAR signaling pathway; cell cycle; arginine and proline metabolism; lysosome; steroid biosynthesis; metabolic pathways; phagosome; biosynthesis of cofactors; riboflavin metabolism; glutathione metabolism; and the Toll-like receptor signaling pathway (Fig. 7).

Validation of genes using q-RT-PCR

To validate the RNA-seq results, six genes with differential expression patterns were randomly selected for examination: *ddx4*, *apoc2*, and *epcam* (upregulated) and *tspan36*, *xdh*, and *tlr7* (downregulated). The expression patterns of all genes were consistent between RNA-seq and RT-PCR results, except for *xdh* (Fig. 8). The fold change represents the ratio of average expression in the PHSA samples compared to the VHSV samples.

In this study, the alignment of gene expression results between RNA-seq and qRT-PCR demonstrated a strong positive correlation ($R^2 = 0.8622$, $p < 0.007$). This correlation indicates that RNA-seq accounted for 86.22% of the variation observed in the qRT-PCR measurements, confirming the consistency and reliability of both techniques. As illustrated in Fig. 9, these findings validate RNA-seq as a robust and comparable method to qRT-PCR for gene expression analysis, providing strong evidence for the successful validation of RNA-seq data in this study.

Gene network prediction

An integrated gene–gene network prediction was conducted using the GeneMANIA prediction server with the database for zebrafish (*Danio rerio*) information (https://genemania.org/) [41]. The input list of significantly differentially expressed genes related to VHS included *TLR7*, *TLR8b*, *TLR2*, *TLR22*, *IRF8*, *IRF7*, *IRF10*, *IRF5*, *IRF6*, *IL12B*, *IL11a*, *IL7R*, *IL1b*, *HSP90B1*, *ENO1*, *TNFa*, *TRF3*, *SPRY1*,

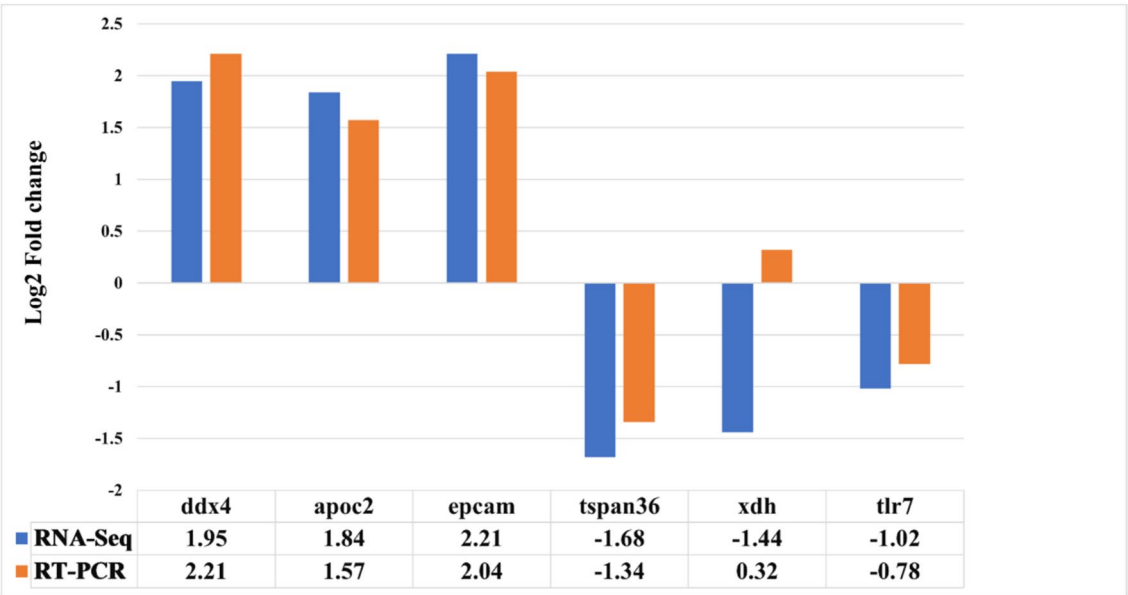

	ddx4	apoc2	epcam	tspan36	xdh	tlr7
RNA-Seq	1.95	1.84	2.21	-1.68	-1.44	-1.02
RT-PCR	2.21	1.57	2.04	-1.34	0.32	-0.78

Fig. 8 Validation of the six genes randomly chosen through RT-PCR, as identified in the RNA-seq analysis of the VHSV and PHSA groups

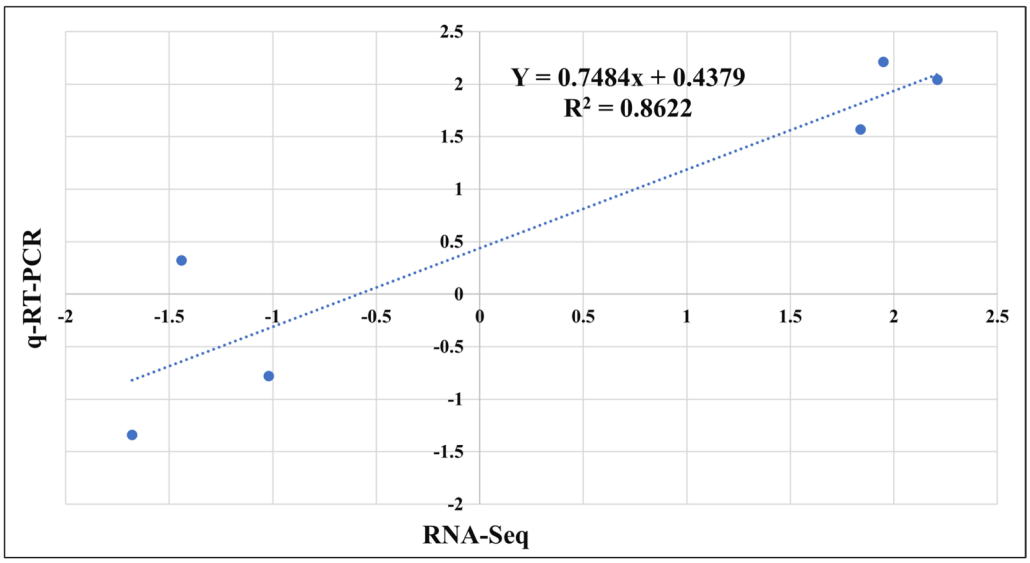

Fig. 9 Correlation between gene expression results in q-RT-PCR and RNA-seq

CASP3, *FN1*, and *GAPDH*. The predicted composite network consisted of 20 hub genes and 21 helper genes, connected by 229 links. The genes were associated with three types of networks: 80.59% shared protein domains, 18.99% co-expression, and 0.41% physical interaction (Fig. 10).

Discussion

Biometric traits

Examining growth and size-related parameters in fish, such as periodic weight gain and changes in body length, provides valuable insights for breeders and the aquaculture industry. In recent years, the import of hatched eggs into Iran has facilitated the spread of the highly contagious viral hemorrhagic septicemia (VHS) disease in rainbow trout (*Oncorhynchus mykiss*) farms, resulting in significant economic losses to the country's fisheries sector [45–48]

The effects of viral injection on fish body weight and length had not been thoroughly investigated prior to conducting this study. The data obtained in this study (Table 2; Supplementary Tables section) demonstrate the significant impact of this disease on fish body weight, indicating a marked effect on their growth and overall weight gain. Although the standard length of the fish did not show significant changes during the first week of the disease challenge, a substantial disparity became evident in the second week. This decline in growth was more pronounced during the second week, suggesting that the virus may impede fish development. Similarly, the disease had a comparable effect on the standard length and fork length of the fish, with infected groups showing a significant reduction in both parameters. While the overall length of the fish remained relatively stable during the first week, a distinct decrease was observed in subsequent weeks, particularly in the virus-infected groups. In conclusion, fish affected by the virus consistently exhibited reduced growth in both weight and length, highlighting the significant economic implications of viral infections for the aquaculture industry.

In Iran, the first reported case of this disease occurred in the northern region of Rudsar, Guilan Province, in 2005. Researchers conducted a comprehensive molecular investigation of Viral Hemorrhagic Septicemia Virus (VHSV) in Iranian rainbow trout (*Oncorhynchus mykiss*) across 100 breeding farms in 10 provinces to identify and diagnose the disease. Tissue samples, including the liver, spleen, kidney, heart, intestine, and pancreas, were collected from VHSV-infected fish for laboratory testing, pathological examination, and molecular analysis. Among the 100 breeding farms surveyed, 15 exhibited positive pathological symptoms, and nested PCR tests confirmed the presence of VHSV in 10 of these farms [45]. The spleen was particularly utilized for diagnosing the disease, yielding positive test results [45].

In another study, samples from VHS-infected fish were collected from six provinces in Iran, regions where rainbow trout is predominantly produced and where the disease exhibits the highest mortality rates. The mass mortality rate in fish farms showing symptoms of the disease ranged from approximately 30% to 70%. The diagnosis of VHS complications was confirmed using RT-PCR. Based on the findings of this study, as well as evidence from previous research on the disease, its origin is believed to lie in European countries [45–48]. Consequently, implementing

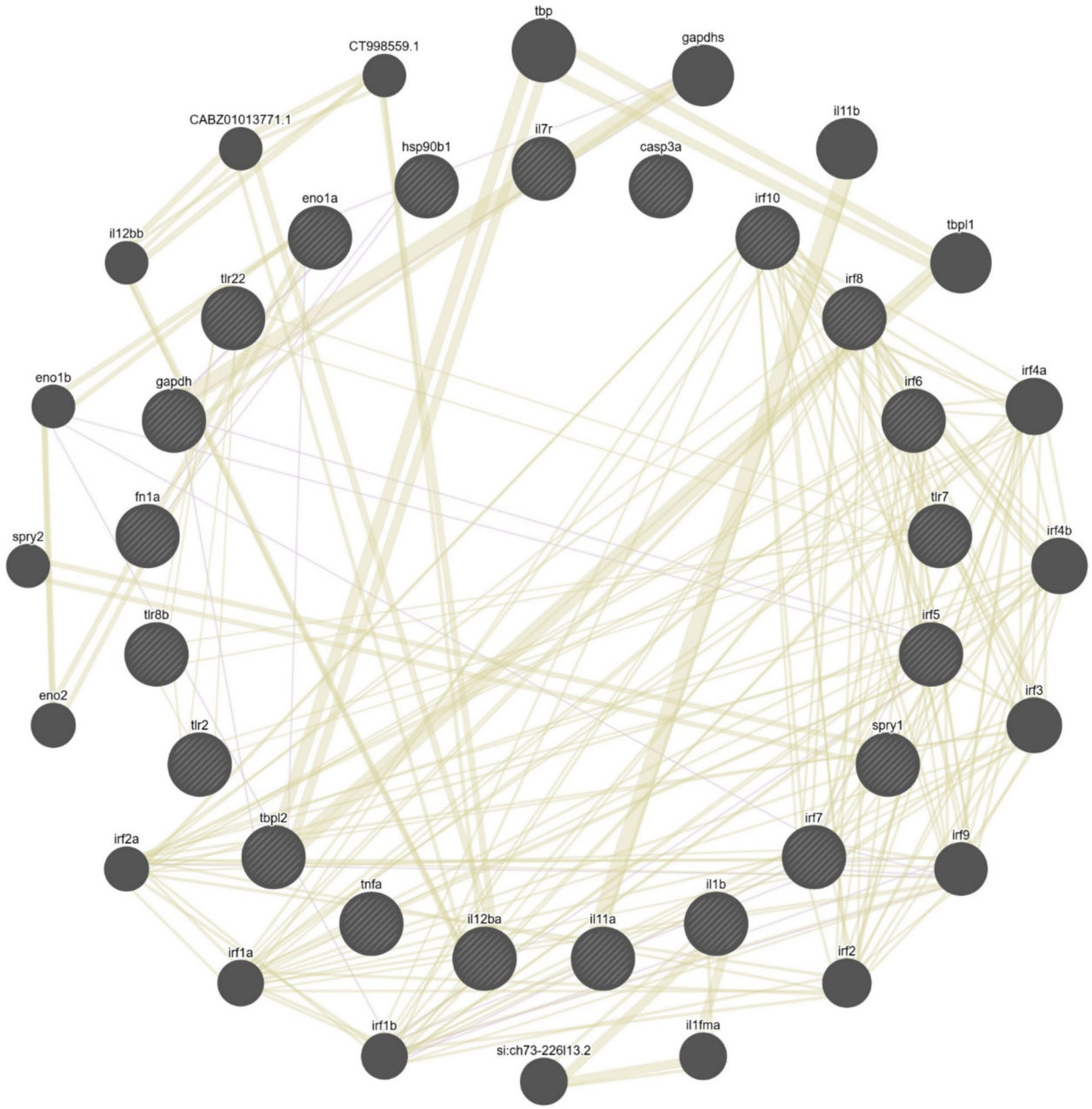

Fig. 10 Predicted gene–gene network of significant DEGs related to VHSV. Striated circles are entry genes and simple circles are helper genes. The size of the genes in the network represents their importance. Yellow connections = shared protein domains; pink connections = physical interactions; purple connections = co-expression

stringent controls and thorough monitoring of imported fish eggs can significantly reduce the impact of the disease and prevent its spread within the country, thereby benefiting fish farms nationwide.

In another study, Viral Hemorrhagic Septicemia (VHS) was investigated in 140 rainbow trout (*Oncorhynchus mykiss*) specimens housed in two separate tanks, designated as the control and treatment groups. Organs, including the kidneys, spleen, heart, skin, liver, pyloric appendages, and brain, were isolated from fish infected with the disease and exhibiting symptoms 12, 13, and 14 days after the experiment began. The findings revealed significant variation in viral load across different organs [47]. In the present study, as in the prior investigation by Fattahi et al. (2019), tissues affected by the disease were isolated within the first week following the challenge.

To assess the level of resistance in rainbow trout (*Oncorhynchus mykiss*) and the expression of the *Mx* gene, various doses of a DNA vaccine (ranging from 10 ng to 10 µg) were administered via intramuscular and intraperitoneal injections to fish weighing 10–100 g. Comparative analysis of these two delivery methods revealed that intraperitoneal vaccination resulted in lower resistance compared to intramuscular injections [49]. In this study, the disease challenge was induced via intraperitoneal injection, which successfully caused the disease in experimental groups A and B. The presence and progression of the disease were confirmed using RT-PCR testing, ensuring the reliability of the research process (see Fig. 1).

The results from the initial and subsequent weeks demonstrated a significant impact of the virus on weight loss in infected fish compared to the control group and those injected with physiological saline. Furthermore, the effect of the virus on body length traits became evident from the eighth day post-injection, with the virus carrier groups exhibiting the lowest growth in length by the end of this period. The findings of this study clearly indicate that the presence of VHSV in rainbow trout (*Oncorhynchus mykiss*) farms adversely affects economic factors such as fish weight and growth, leading to substantial financial losses for breeders. Therefore, by replicating and validating these findings and promoting their outcomes, it is possible to raise awareness among industry stakeholders about the importance of adhering to health protocols and implementing preventive measures in breeding farms. Such actions could significantly mitigate the economic consequences of the disease. Additionally, systematic and rigorous monitoring of the importation of hatched eggs from international sources could play a pivotal role in improving the health standards of rainbow trout breeding operations.

Based on the observed changes in fish weight and length following infection, this study suggests that VHSV not only directly impacts immunity but also indirectly affects fish growth and development. Furthermore, these findings underscore the significance of biological pathways and highlight the critical need to incorporate genetic resistance into breeding programs. By identifying key genes and regulatory mechanisms associated with VHSV resistance, this study provides a foundation for the development of molecular tools aimed at enhancing disease resistance in rainbow trout (*Oncorhynchus mykiss*).

Bioinformatic analysis

Analysis of the sequencing results identified 1,726 genes with significant differential expression between the physiological saline and virus-injected groups. Among these, the differential expression of genes such as *cyr61*, *hsp90aa1.2*, *hsp90b1*, *irf10*, and *cdk1* aligns with the findings of Verrier et al. (2018) [5]. Deciphering antiviral response mechanisms is essential for mitigating the effects of VHSV in fish as it uncovers host–pathogen dynamics and identifies immune markers and gene expression profiles vital for resistance breeding and sustainable aquaculture [50]. The immune response of fish to viral infections begins with innate immune activation, progressing to antibody production and cytotoxic T-cell activity [50–53].

This section explores key genes, including *TLR2*, *TLR7*, *TLR8*, *TLR22*, *IRF5*, *IRF6*, *IRF7*, *IRF8*, *IRF10*, *IL11a*, *IL12B*, *IL1b*, *IL7R*, *ILR1 II*, *HSP90B1*, *HSP47*, *TNF-α*, *TRF3*, *SPRY1*, *CASP3*, FN1, *GAPDH*, and *IgGFc-binding proteins*, focusing on their functions and significance. Their roles in cellular processes, immune responses, and molecular mechanisms related to VHSV are analyzed. The *TLR* (Toll-like receptor) gene family, particularly *TLR7*, plays a crucial role in immune responses to viral infections such as VHSV in fish. *TLR7* recognizes viral ribonucleic acids, triggering the secretion of type I interferons to initiate antiviral defense mechanisms. It regulates immune gene activity, predominantly in dendritic and B cells, which are essential for VHSV recognition. *TLR7* expression varies across cellular phenotypes, with elevated levels observed in immune cell populations. Understanding the activation of *TLR7* during VHSV infection in fish provides valuable insights into enhancing immune resilience and viral resistance [54]. A detected reduction in *TLR7* expression (log2 fold change = −1.02) suggests a potential alteration of the innate immune response during VHSV infection. This reduction may represent a viral strategy to evade host defenses by suppressing antiviral mechanisms. Confirmed through qPCR (log2 fold change = −0.78), this observation underscores the critical role of TLR7-mediated pathways in immune function and highlights *TLR7* as a promising molecular target for improving resistance to viral infections in rainbow trout.

TLR7 and *TLR8* are critical for the detection of viral RNA and the activation of immune defenses. TLR7's capacity to recognize single-stranded RNA (ssRNA) from RNA viruses underscores its pivotal role in combating VHSV. Upon recognizing viral RNA, TLR7 initiates signaling pathways that stimulate the production of interferons, particularly type I interferons (IFNs), which are essential antiviral mediators in fish [55]. *TLR8*, sharing structural and functional similarities with *TLR7*, also interacts with ssRNA and plays a complementary role in amplifying the antiviral immune response. In rainbow trout (*Oncorhynchus mykiss*), these receptors contribute to the upregulation of antiviral genes and proteins, thereby strengthening the host's defenses against VHSV infection [56].

The release of type I interferons, which are key antiviral defenses of the body, is significantly stimulated by *TLR7*. Expression levels of *TLR7* vary across different cell types. In both humans (*Homo sapiens*) and mice (*Mus musculus*), dendritic cells and B cells demonstrate predominant expression of the *TLR7* gene [43]. Furthermore, *TLR7* and *TLR8*, previously associated with disease resistance, exhibited significant differential expression. Additionally, novel genes such as *ifn1-202* (interferon α3-like), *ifnphi3* (interferon β-like), and *irf8* (interferon regulatory factor 8) were identified as critical components of the type I IFN pathway, as highlighted in prior research [5].

Toll-like receptor (TLR) genes play a critical role in VHSV infection in rainbow trout (*Oncorhynchus mykiss*), facilitating pathogen recognition and initiating immune responses in rainbow trout and other fish species. These receptors are integral components of the innate immune system, responsible for activating inflammatory and adaptive immune responses by recognizing conserved pathogen-associated molecular patterns. Upon detecting pathogens, TLRs activate signaling cascades that trigger inflammation and subsequently stimulate adaptive immunity [57–59]. *TLR2* specifically recognizes a broad range of microbial ligands, including components from bacteria, fungi, and viruses. During VHSV infection in rainbow trout, *TLR2* is essential for early viral detection. It binds to viral components on immune cells, initiating an inflammatory response. This response involves the activation of key cytokines such as *IL-1* and *TNF-α*, which act as primary mediators in controlling the infection and recruiting immune cells to the site of infection [58]. The role of *TLR2* in detecting pathogen-associated molecular patterns, particularly from VHSV, has been well-documented in scientific research [60].

TLR22 detects RNA viruses such as VHSV in fish and activates immune signaling pathways involving *NF-κB* and *AP-1*. This activation promotes the production of cytokines and antiviral genes, enabling the host to combat the infection [55]. In rainbow trout (*Oncorhynchus mykiss*), *TLR22* plays a pivotal role in initiating the immune response to VHSV by activating innate pathways and inducing the secretion of cytokines and interferons [56].

Transcriptomic data from rainbow trout infected with VHSV provide valuable insights into how TLRs regulate immune responses. Analysis of gene roles and expression changes associated with TLR signaling pathways revealed that *TLR2*, *TLR7*, *TLR8*, and *TLR22* modulate immune activity at the transcriptional level. The activation of these TLRs enhances immune gene expression, thereby promoting an effective defense against the virus.

The expression of immune-associated genes in response to viral pathogens such as VHSV has been extensively characterized in fish models. Several key interferon regulatory factors (IRFs) play a pivotal role in orchestrating immune responses during viral infections. For instance, in zebrafish (*Danio rerio*), the activation of *IRF5* and *IRF7* is linked to the regulation of innate immune functions during *Mycobacterium marinum* infections [61].

IRF5 is specifically induced in macrophages upon infection, underscoring its critical role in the early stages of immune defense. *IRF7* and *IRF8* are key regulators of type I interferon synthesis, which is essential for controlling viral replication and initiating immune responses. During infection with various pathogens, including VHSV, the upregulation of these genes highlights their involvement in regulating immune responses during viral infections [62].

Further studies indicate that *IRF5* and *IRF7* are upregulated during viral stress in fish, demonstrating their critical role in type I interferon production. This activation is essential for the host's defense mechanisms against viral infections such as VHSV. Although a connection between *IRF6* and immune responses has been observed, its specific role in viral infections remains poorly understood. *IRF6* is thought to regulate cellular stress responses and may contribute to early immune defense during infections like VHSV by maintaining epithelial tissue integrity [63].

Additional transcriptomic studies have shown that *IRF7* and *IRF8* are significantly upregulated in zebrafish (*Danio rerio*) following infections with *Salmonella* and *Mycobacterium* [64]. *IRF8*, in particular, plays a key role in activating genes involved in pathogen recognition and inflammatory responses, mirroring its function in mammals. These findings emphasize the critical role of IRF family members in modulating innate immune responses during infection. Although *IRF10* has been less extensively studied in fish models, it is believed to contribute to antiviral responses, underscoring the need for further research to clarify its role in regulating immune defenses during VHSV infection [65].

The upregulation of *IRF5*, *IRF7*, and *IRF8* during VHSV infection in rainbow trout (*Oncorhynchus mykiss*) underscores their critical roles in regulating immune pathways for viral defense. These genes are involved in the activation of interferon-mediated immune responses, which are essential for controlling viral replication. The increased expression of *IRF8* following infection suggests its significant contribution to the innate immune response to pathogen-associated molecular patterns (PAMPs) from VHSV [66]. Although *IRF10* has not been directly identified in rainbow trout during VHSV infection, its role in immune responses in other vertebrates suggests it may contribute to broader immune regulation during viral

infections [67]. Collectively, IRF family members including *IRF5*, *IRF7*, *IRF8*, and potentially *IRF10* play essential roles in managing immune responses during VHSV infection in rainbow trout. These genes are crucial for the production of type I interferons and pro-inflammatory cytokines, which regulate viral replication and initiate immune defense mechanisms. Further research is needed to elucidate the specific roles of these IRF genes in fish immune responses, particularly their interactions with other immune components, to ensure effective defenses against viral pathogens such as VHSV [68, 69].

The roles of immune-related genes, such as *IL11a*, *IL12B*, *IL1b*, *IL7R*, and *ILR1 II*, in VHSV-infected rainbow trout (*Oncorhynchus mykiss*) are critical for modulating immune responses. Among these, *IL11a* plays a particularly significant role in inflammation and immune regulation. In various fish species, *IL11a* has been shown to trigger the production of inflammatory cytokines, contributing to the acute-phase response during infection. Its expression typically increases during viral infection, indicating its involvement in the host's defense against viral pathogens such as VHSV. Within signaling pathways, *IL11a* recruits immune cells, including neutrophils and macrophages, which are essential for combating viral infections. Understanding the function of *IL11a* in the context of VHSV infection could provide valuable insights into how fish initiate immune responses to limit viral replication and spread. Such findings align with ongoing efforts to link gene expression data to the mechanisms underlying VHSV infection. [70–72].

IL12B, a cytokine involved in immune regulation, plays a crucial role in inducing T-helper 1 (Th1) responses. During VHSV infection, *IL12B* activates natural killer (NK) cells and T cells, both of which are essential for an effective immune response. Its increased expression in infected fish highlights its role in enhancing host antiviral defenses. *IL12B* promotes the secretion of interferon-gamma (*IFN-γ*), a potent antiviral cytokine that stimulates immune cell activity and facilitates pathogen clearance. Furthermore, the upregulation of *IL12B* may drive immunity toward Th1-mediated responses, which are critical for controlling VHSV and other viral infections. These findings support the hypothesis that transcriptome data can provide valuable insights into the mechanisms underlying infection and immune responses [70–72].

The gene *IL1b* plays a pivotal role in the inflammatory response during VHSV infection. By activating immune cells and promoting the production of other cytokines, *IL1b* amplifies the immune response. In rainbow trout (*Oncorhynchus mykiss*), *IL1b* expression is typically elevated in response to various pathogens, including VHSV. Its role in inducing fever and stimulating the production of acute-phase proteins highlights its significance in the systemic immune response. Additionally, *IL1b* helps balance pro-inflammatory and anti-inflammatory signals through interactions with other cytokines, ensuring a well-regulated immune response. The upregulation of *IL1b* during VHSV infection may provide insights into the activation of inflammatory pathways essential for pathogen control and clearance. The involvement of this gene underscores the critical role of immune regulation in viral infections [73].

IL7R and *ILR1 II* play crucial roles in regulating lymphocyte differentiation and activation, which are essential components of the adaptive immune response in fish. *IL7R* supports T-cell survival and proliferation, both critical for effective adaptive immunity. During VHSV infection, *IL7R* expression is upregulated, likely enhancing T-cell-mediated responses to combat the virus. Similarly, *ILR1 II*, a cytokine receptor, facilitates immune activation by mediating signaling pathways involving various cytokines critical for antiviral defense. The increased expression of these genes in response to VHSV infection may reflect the host's effort to strengthen immune memory and improve long-term resistance. Linking these gene expression changes with transcriptomic data provides valuable insights into the complex interplay between gene regulation and immune responses during VHSV infection [74–77].

This study examined the roles of key immune-related genes, including *HSP90B1*, *HSP47*, and *TNF-α*, in the response of rainbow trout (*Oncorhynchus mykiss*) to VHSV infection. Given the impact of VHSV infection on immune pathways, understanding the functions of these proteins provides valuable insights into the defense mechanisms of fish.

HSP90, particularly its isoform *HSP90B1*, plays a critical role in maintaining cellular homeostasis and facilitating the cellular stress response during VHSV infection. Under normal conditions, 5–10% of *HSP90* localizes to the cell nucleus, with this proportion increasing under heat stress [78, 79]. This suggests that during VHSV infection, the enhanced nuclear localization of *HSP90B1* may support crucial immune-related processes such as transcriptional regulation and cell cycle progression. *HSP90B1* binds to DNA, RNA, and histones, thereby modulating DNA structure and contributing to RNA synthesis and processing-functions essential for maintaining cellular integrity under stress [80]. These mechanisms are particularly critical during infection, enabling the expression of immune-related genes and ensuring the proper function of immune cells. Additionally, *HSP90B1* associates with nucleoli and perichromatin ribonucleoprotein fibrils [81, 82], underscoring its role in regulating RNA synthesis and its potential influence on the expression of

immune response genes that are upregulated during viral infections.

HSP47, a key protein in collagen biosynthesis, plays a critical role in managing stress responses during inflammation and tissue damage caused by viral infections such as VHSV. *HSP47* regulates collagen folding and secretion, ensuring the proper conformation of newly synthesized collagen [83]. Its involvement in collagen synthesis is closely tied to the tissue remodeling processes that occur during infection and inflammation. Dysregulation of *HSP47* can lead to fibrosis or excessive collagen deposition, conditions often observed in chronic viral infections. Additionally, *HSP47* protects collagen from misfolding and aggregation, particularly under the oxidative stress experienced by fibroblasts during infection [83]. These mechanisms are particularly relevant during VHSV infection, as the virus induces inflammation and cellular stress, compromising connective tissue integrity and driving pathological changes.

TNF-α plays a critical role in the immune response to VHSV infection, regulating inflammation and cell survival. As a central mediator of inflammation, its expression is tightly controlled in immune cells and tissues [78]. In response to infection, *TNF-α* activates multiple pathways, including *NF-κB*, to modulate immune gene expression related to inflammation, apoptosis, and cell survival. These pathways are essential for mounting a robust immune response against viral infections. *TNF-α* stimulates transcription factors such as *NF-κB* and *AP-1*, which are crucial for initiating inflammatory gene expression and ensuring cellular survival under stress conditions [84]. During VHSV infection, increased *TNF-α* expression may enhance the inflammatory response and promote viral clearance. However, excessive or unregulated TNF-α activity can also contribute to tissue damage and apoptosis. Additionally, *TNF-α* influences apoptotic pathways by activating caspases and other downstream effectors [84], affecting the fate of infected cells and facilitating viral clearance. This dual role underscores the importance of *TNF-α* in both defending the host through immune responses and potentially contributing to tissue pathology if its expression is not properly regulated during prolonged viral infection.

In summary, the expression profiles of *HSP90B1*, *HSP47*, and *TNF-α* are critical to the response of rainbow trout (*Oncorhynchus mykiss*) to VHSV infection. These proteins regulate immune responses and influence stress and tissue repair mechanisms, both of which are pivotal during viral infections. The upregulation of these genes during infection highlights a complex interplay between cellular stress responses and immune activation, contributing to both viral clearance and the pathophysiological changes observed in infected fish.

The *TRF3* gene encodes a transcription factor similar to *TBP* (TATA-binding protein), which is critical for forming the preinitiation complex required for RNA polymerase II transcription in eukaryotic organisms. Genomic analyses have identified the *TRF3* sequence on human chromosome 14, revealing high similarity to the conserved C-terminal region of TBP, suggesting functional parallels with other TBP-related factors (TRFs) such as *TRF1* and *TRF2*. While *TRF2* interacts with general transcription factors *TFIIA* and *TFIIB*, it does not bind the TATA box due to differences in its DNA-binding domain. Similarly, *TRF3* is thought to contribute to transcription regulation and the diversity of the general transcription machinery. However, its specific roles in transcription initiation and potential tissue-specific expression, similar to the function of *TRF1* in *Drosophila melanogaster*, remain to be elucidated and warrant further investigation [85].

CASP3 (Caspase-3) plays a critical role in both apoptotic and non-apoptotic functions within the immune response, particularly during viral infections such as VHSV. Caspases are highly conserved cysteine-dependent proteases that are essential for mediating apoptosis and inflammatory responses [86]. As an executioner caspase, *CASP3* is well-known for its involvement in programmed cell death, but its functions extend beyond apoptosis. Caspases, including *CASP3*, are now recognized as key players in non-apoptotic signaling pathways, regulating various cellular and physiological processes [87–89]. Recent studies have shown that *CASP3* influences several physiological responses, including immune system regulation and tissue repair, by modulating cellular differentiation, migration, and survival [87–91]. During VHSV infection in rainbow trout (*Oncorhynchus mykiss*), *CASP3* may regulate immune cell apoptosis and inflammation while supporting the repair of damaged tissues through its non-apoptotic roles [92]. This dual functionality is particularly relevant during viral infections, where the immune response triggered by the virus likely activates *CASP3*, affecting both cellular defense mechanisms and recovery processes [93]. Separately, the *TRF3* gene encodes a transcription factor similar to TBP (TATA-binding protein), which is critical for assembling the preinitiation complex required for RNA polymerase II transcription in eukaryotic cells [94].

Sequencing data revealed distinct immune responses in rainbow trout (*Oncorhynchus mykiss*) during VHSV infection. In a study by Verrier et al. (2018) [5], the type I interferon (IFN) pathway was strongly associated with resistance in the B57 line, highlighting its critical role in antiviral defense. Similarly, key pathways such as *Jak-STAT* signaling, *MAPK* signaling, and cytokine-cytokine interactions were identified in both the present study

and that of Verrier et al. (2018), underscoring their central roles in coordinating immune responses. The resistant *B57* line exhibited enhanced activation of metabolic and immune pathways, consistent with the robust glycerophospholipid metabolism and cytokine-cytokine interaction pathways discussed by Verrier et al. (2018) [5]. In contrast, the *A22* cell line showed upregulated apoptosis and cell cycle pathways, suggesting increased cellular stress and viral manipulation. These findings align with the apoptosis and *p53* signaling pathways identified in Verrier et al. (2018) [5]. Both studies highlighted *rsad2*, *vig1*, and *mxa* as key differentially expressed genes, emphasizing their pivotal roles in antiviral immunity. Thus, while the present results confirm the immune regulatory mechanisms observed by Verrier et al. (2018) [5], they also underscore the distinct host responses that determine resistance or susceptibility to VHSV.

Transcriptome analysis of fish lines that are either susceptible or resistant to disease has provided valuable insights into the immune response to viral infections, particularly VHSV in rainbow trout (*Oncorhynchus mykiss*). A study focusing on two key tissues, the spleen and anal fin, revealed distinct gene expression profiles between disease-susceptible and disease-resistant fish lines. The disease-sensitive group exhibited a greater number of differentially expressed genes compared to the resistant group, suggesting a heightened immune response or possible dysregulation during infection [95]. Variations in gene expression, especially in immune-related genes, underscore the role of innate immunity in determining host susceptibility to VHSV, as supported by previous research on fish immune systems [95]. The present study identified the activation of pathways such as Toll-like receptor signaling and *p53* signaling, suggesting their potential involvement in viral resistance.

Additionally, a correlation was observed between the presence of *neurorhabdoviruses* in anal fin tissue and survival rates during initial viral replication, further emphasizing the importance of tissue-specific immune responses during infection [95]. This study identified 1,726 differentially expressed genes, which contrasts with findings from a previous study [95] that reported 19,324 differentially expressed genes in spleen tissue from the disease-sensitive group (compared to the control group) and 593 differentially expressed genes in the spleen tissue from the resistant group (compared to the control group). The differences in gene expression observed in this study may stem from variations in fish breeds, breeding and maintenance conditions (including differences in water quality and feeding practices), the absence of differentiation or detection of resistance and sensitivity in the two research groups, the type of experimental challenge (e.g., peritoneal injection with a vaccine), differences in sampling times, tissue selection, and biological factors affecting the body and tissues in each study. Additionally, differences in sequencing platforms and methodologies may have contributed to the observed discrepancies.

The findings of this study align with the idea that VHSV infection triggers a complex immune response in rainbow trout, involving the regulation of multiple immune pathways to combat viral threats. It is crucial to recognize that the sensitivity of fish to VHSV infection may depend on the efficient regulation of these pathways, providing valuable insights for future aquaculture breeding strategies aimed at enhancing disease resistance. These results offer a detailed understanding of the molecular mechanisms underlying the immune response to VHSV infection in rainbow trout, highlighting the need for further research into immune pathway regulation to mitigate the impact of the virus in aquaculture.

Through the examination and analysis of genetic and transcriptomic data on VHSV infection in two rainbow trout (*Oncorhynchus mykiss*) lines-one sensitive (*A22*) and one resistant (*B57*) researchers identified a QTL associated with resistance in the isogenic fish line *B57* and high sensitivity in line *A22*. This QTL was found to be effective not only during viral challenges administered via immersion but also during injection challenges. Sequencing results revealed that cell lines derived from the *B57* and *A22* fish lines exhibited an enhanced reaction to inactivated VHSV virus inoculation. Furthermore, by crossing the backcross hybrid of the isogenic lines with the parental line, the associated QTL was mapped to chromosome 3. Significant biological pathways identified in the resistant line *B57*, based on the KEGG database, included glycerophospholipid metabolism, cytokine-cytokine interactions, *Jak-STAT* signaling, fructose and mannose metabolism, endocytosis, *MAPK* signaling, and other metabolic pathways. These pathways are significant as they collectively enhance antiviral defense, immune signaling, metabolic adaptation, and cellular stress responses, contributing to VHSV resistance in the B57 line. In contrast, the KEGG pathways in the sensitive line *A22* included fructose and mannose metabolism, biosynthesis of unsaturated fatty acids, oocyte maturation, progesterone signaling, sphingolipid metabolism, fatty acid metabolism, glutathione metabolism, inositol phosphate metabolism, *p53* signaling, cell cycle, apoptosis, and purine metabolism. The identification of the type I interferon (IFN) gene was highlighted as a critical factor in the differential response to VHSV between the resistant and sensitive fish lines. Key differentially expressed genes identified in this study included *rsad2*, *vig1*, *mxa*, *igs15*, *pcdh10*, *cyr61*, *hsp90*, *dhx58*, *irf1*, *cd9*, *ogfr*, *cyp1B1*, and *akr1b1*. Among these, the type I IFN pathway was identified as one of the main pathways involved in the

immune response to VHSV. Additionally, the *crfb1* gene was recognized as playing an important role within this pathway [5].

In one study, researchers investigated and characterized QTLs associated with resistance to VHS disease in rainbow trout (*Oncorhynchus mykiss*), a significant threat to the aquaculture industry in Europe [96]. Maintaining animal health and controlling diseases are critical components of aquaculture, and understanding the genetic basis of disease resistance in species such as fish is essential. Identifying QTLs for specific traits enhances our understanding of the genetic architecture underlying important characteristics and provides valuable insights into the mechanisms of pathogen resistance. This study utilized the *F2* generation of rainbow trout families to identify QTLs. Ultimately, the researchers identified seven QTLs associated with survival, with one QTL accounting for 65% of the survival variation across the genome [96].

The findings of this study highlight the critical role of innate immunity in viral resistance and present opportunities to identify key genes associated with this process. The identification of genes with significant effects provides a valuable framework for selecting and breeding disease-resistant fish. Notably, one of the QTLs linked to disease resistance was located near the *Mx* gene, which belongs to the interferon-stimulated gene family and is known for its role in innate antiviral immune responses. Polymorphisms in *Mx* sequences have also been associated with resistance to other *rhabdoviruses*, including *IHNV*. Although the precise position of the fibronectin gene remains unclear, the data suggest that it likely contributes to one of the most effective QTL regions for disease resistance. Genes involved in activating the *IFN* system were identified as crucial factors in developing resistance in this study. Additionally, the Toll-Like Receptor (TLR) signaling pathway was recognized for its role in producing proteins essential for innate immunity. Specifically, *TLR7* and *TLR8* were identified as key candidate genes influencing QTL regions. Furthermore, *SPRY* was found to play a role in immune defense mechanisms, while the trim13 gene, which is associated with cellular stress in mammals, was shown to be closely related to *spryd7* in fish and other vertebrate genomes [96].

In the current study, although no major genes or QTLs were specifically identified, the gene expression profiles of all genes were analyzed. Certain genes associated with or located near QTLs, such as *TLR7* and *TLR8*, which were identified in a previous study [96], were also detected in this investigation and included among the notable genes exhibiting differential expression. Consistent with prior research, findings from this transcriptome analysis revealed the presence of interferon genes (*ifn1-202*, *ifnphi3*, *irf7*, and *irf8*) among the primary and significant genes. These genes were differentially expressed in both the physiological serum and viral groups. Additionally, when examining the major biological and metabolic pathways identified in this study, the Toll-Like Receptor (TLR) signaling pathway was highlighted in the KEGG database. This pathway consisted of 12 genes and demonstrated a significantly corrected *P*-value, underscoring its relevance in the context of immune responses during viral infections.

The rhabdovirus family comprises two primary groups, VHSV and IHNV, both of which cause high mortality rates and significant economic losses in the aquaculture industry. Studies examining these diseases in rainbow trout (*Oncorhynchus mykiss*) have established that there is no substantial correlation between them. Furthermore, it has been demonstrated that body weight plays a crucial role in IHNV susceptibility and disease severity. Statistical analyses revealed that juvenile fish with lower body weights were more susceptible to infection than adult fish. Fish weighing less than one gram exhibited notably higher susceptibility to viral infections, with individuals averaging 0.43–0.44 g being 87 times more susceptible to the disease than those averaging 2.5 g. Similarly, a review of various studies indicated a very limited correlation between these two viral diseases. Investigations into the quantity and levels of glycoproteins in salmon)*Oncorhynchus*(revealed that these proteins significantly influence the relative resistance of fish to *rhabdoviruses*. Specifically, fibronectin, an extracellular glycoprotein, facilitates the entry of VHSV and other rhabdoviruses, such as IHNV, into fish cells. Fibronectin is also a target of protective neutralizing antibodies [97]. In this study, fish weights across different groups were standardized, and only variations in body weight and length were analyzed. By the first week after viral challenge (day 28), fish challenged with the virus exhibited significant weight changes compared with the control group ($p < 0.01$). Additionally, fish injected with the virus displayed weight differences compared with those receiving saline injections ($p < 0.05$). By the second week after the challenge (day 35), a significant difference in body weight was observed between the septicemia injection groups and the other experimental groups, including the control and saline injection groups ($p < 0.001$). Significant differences in fish length traits (standard length, fork length, and total length) were also noted among the experimental groups during the second week post-challenge ($p < 0.05$). These findings suggest that VHS disease can significantly impair fish growth, leading to economic losses. Furthermore, consistent with the findings of

[97], transcriptome analysis in this study identified the fibronectin 1 gene as exhibiting significant differential expression, further validating prior research.

Validation of RNA-seq analysis

qRT-PCR is widely used as a validation tool to confirm gene expression results obtained from next-generation sequencing (NGS). In this study, relative quantification of gene expression of six immunomodulatory genes (*ddx4*, *apoc2*, *epcam*, *tspan36*, *xdh*, and *tlr7*) was assessed through transcriptome analysis to elucidate the gene expression profile of the immune response. Among these genes, *ddx4*, *apoc2*, and *epcam* were upregulated, while *tspan36*, *xdh*, and *tlr7* were downregulated. The qRT-PCR results were consistent with the sequencing data for all tested genes, except for *xdh*, which showed an inverse correlation. In a previous study [5], the relative expression of six genes (*cd9*, *fosl*, *ifi44*, *irfb1*, *irf7*, and *rsad2*) was validated at three and six days post-challenge compared to the control group. Although gene expression efficiency in the qRT-PCR analysis was estimated at approximately 86%, no direct comparison of expression levels between sequencing and qRT-PCR methodologies was conducted, which could provide additional insights into potential discrepancies.

Conclusions

This study investigated the effects of viral infection on various biometric parameters in rainbow trout (*Oncorhynchus mykiss*) across five treatment groups. Body weight analysis during the first week of the viral challenge revealed significant differences between the virus-injected groups and both the control and physiological saline-injected groups. By the second week, the virus-injected groups showed significant reductions in body weight compared to the other experimental groups. While no significant differences in standard length, fork length, and total length were observed during the first week, notable variations emerged in the second week across the experimental groups. These findings demonstrate that VHSV impairs fish growth, posing substantial economic risks to aquaculture. Given the lack of an effective cure for VHSV, strict adherence to health standards and preventive measures is critical. Future research should prioritize gene expression profiling and spleen tissue analysis in rainbow trout (*Oncorhynchus mykiss*). RNA sequencing identified 1,726 differentially expressed genes, including immune-related genes such as *TLR7*, *TLR8*, and various interleukins. Gene network analysis revealed complex interactions among genes, implicating significant metabolic pathways, including the *P53* signaling pathway, Toll-like receptor signaling pathway, and apoptosis pathway. QTLs associated with VHSV resistance were linked to *TLR7* and *TLR8*. Real-time PCR validation of RNA-seq results for six selected genes confirmed the reliability of most findings. Bioinformatic analysis further identified key biomarker genes, offering significant potential for inclusion in breeding programs aimed at enhancing the resistance of rainbow trout (*Oncorhynchus mykiss*) to VHSV.

Supplementary Information

The online version contains supplementary material available at https://doi.org/10.1186/s12864-025-11300-x.

Supplementary Material 1.
Supplementary Material 2.
Supplementary Material 3.
Supplementary Material 4.
Supplementary Material 5.

Acknowledgements

The authors extend their gratitude to the following individuals and organisations: Mr. Davood Saneei, a member of the Board of Directors of Mobarak Andish Advanced Technologies, for his financial support. Sari Agricultural Sciences and Natural Resources University for providing financial support and laboratory facilities. The Iran Veterinary Organization for supplying the virus. Dr. Arman Ghorbanzadeh and Mr. Seyyed Ahmad Mashhadi for their invaluable assistance in addressing the practical challenges associated with the disease. Mr. Ehsan Amiri, a prominent breeder, for sourcing the rainbow trout from Al-Shatar Farm.

Authors' contributions

M.G. managed the project, overseeing fish breeding, sample collection, RNA extraction, subsequent cDNA synthesis, and quantitative RT-PCR analyses. Then M.G. performed the complete RNA-seq data analysis, conducted biometric and statistical analyses, and was responsible for writing and editing the manuscript. G.R. provided project leadership and guidance, including the design of the methodology, and co-authored and edited the manuscript. A.N. led the project, designed the scientific and practical methodology, and secured funding from the private investor. N.S. facilitated the experimental challenge by securing and preparing the venue, procuring VHSV from the Iran Veterinary Organization, implementing the challenge protocol, and ensuring experimental biosafety.

Funding

This work was supported by Mobarak Andish Advanced Technologies, a leading animal-breeding company in Iran, and the Sari Agricultural Sciences and Natural Resources University.

Data availability

The datasets generated during the current study are are available at the NCBI (BioProject PRJNA1134344, https://www.ncbi.nlm.nih.gov/sra/PRJNA1134344).

Declarations

Ethics approval and consent to participate

All animals and experimental protocols adhered to the guidelines for the care and use of fish in research, as approved by the Ethics Committee of the Iran Veterinary Organization, Department of Aquatic Animal Health and Disease (Approval Code: 96–40-75133). In the practical part of the experiment, to minimize animal distress and ensure their welfare during the experimental challenge, virus inoculations were performed under light anesthesia with the chosen substances and dosages. Fish in different groups, including

those injected with VHSV, the control group (without injection), and the group injected with PHSA, were anesthetized and handled in an immersion bath containing 100 mg/L of a 10% eugenol solution[98, 99]. Fish exhibiting signs of clinical disease (mortality, exophthalmia, hemorrhaging, anemia, and abnormal behavior involving spiral swimming) underwent intensive monitoring, with checks occurring at least three times a day. Regular water quality checks ensured a clean environment for the fish during the infectious challenge. Dead fish and those displaying signs of distress (swimming abnormally) were promptly removed. After a two-week injection challenge, fish from different groups were observed for clinical symptoms. Disease diagnosis was confirmed via RT-PCR. Subsequently, all fish were humanely euthanized using a lethal dosage of 600 mg/L of a 10% eugenol solution in an immersion bath, adhering to animal welfare guidelines [100–102].

Consent for publication
Not applicable.

Competing interests
The authors declare no competing interests.

Author details
[1]Laboratory for Molecular Genetics and Animal Biotechnology, Faculty of Animal Sciences and Fisheries, Sari Agricultural Sciences and Natural Resources University, Sari, Iran. [2]Department of Animal Science, University College of Agriculture and Natural Resources, University of Tehran, Karaj, Iran. [3]Aquatic Animal Health and Diseases Management Department, Iranian Veterinary Organization, Tehran, Iran.

Received: 2 July 2024 Accepted: 29 January 2025
Published online: 28 February 2025

References

1. Panzarin V, Cuenca A, Gastaldelli M, Alencar ALF, Pascoli F, Morin T, Blanchard Y, Cabon J, Louboutin L, Ryder D, et al. VHSV Single Amino Acid Polymorphisms (SAPs) Associated With Virulence in Rainbow Trout. Front Microbiol. 2020;11:1984.
2. Walker PJ, Winton JR. Emerging viral diseases of fish and shrimp. Vet Res. 2010;41(6):51.
3. Kim R, Faisal M. Emergence and resurgence of the viral hemorrhagic septicemia virus (Novirhabdovirus, Rhabdoviridae, Mononegavirales). J Adv Res. 2011;2(1):9–23.
4. Lafferty KD, Harvell CD, Conrad JM, Friedman CS, Kent ML, Kuris AM, Powell EN, Rondeau D, Saksida SM. Infectious diseases affect marine fisheries and aquaculture economics. Ann Rev Mar Sci. 2015;7:471–96.
5. Verrier ER, Genet C, Laloë D, Jaffrezic F, Rau A, Esquerre D, Dechamp N, Ciobotaru C, Hervet C, Krieg F, et al. Genetic and transcriptomic analyses provide new insights on the early antiviral response to VHSV in resistant and susceptible rainbow trout. BMC Genomics. 2018;19:482.
6. Crane M, Hyatt A. Viruses of fish: An overview of significant pathogens. Viruses. 2011;3(11):2025–46.
7. Baillon L, Mérour E, Cabon J, Louboutin L, Vigouroux E, Alencar ALF, Cuenca A, Blanchard Y, Olesen NJ, Panzarin V, et al. The Viral Hemorrhagic Septicemia Virus (VHSV) Markers of Virulence in Rainbow Trout (Oncorhynchus mykiss). Front Microbiol. 2020;11:574231.
8. Henryon M, Berg P, Olesen NJ, Kjær TE, Slierendrecht WJ, Jokumsen A, Lund I. Selective breeding provides an approach to increase resistance of rainbow trout (Onchorhynchus mykiss) to the diseases, enteric redmouth disease, rainbow trout fry syndrome, and viral haemorrhagic septicaemia. Aquaculture. 2005;250(3):621–36.
9. Ammayappan A, Vakharia VN. Molecular characterization of the great lakes viral hemorrhagic septicemia virus (VHSV) isolate from USA. Virol J. 2009;6:171. https://doi.org/10.1186/1743-422X-6-171.
10. Schütze H, Enzmann PJ, Mundt E, Mettenleiter TC. Identification of the non-virion (NV) protein of fish rhabdoviruses viral haemorrhagic septicaemia virus and infectious haematopoietic necrosis virus. J Gen Virol. 1996;77(Pt 6):1259–63.
11. Sepúlveda D, Lorenzen N. Can VHS virus bypass the protective immunity induced by DNA vaccination in rainbow trout? PLoS ONE. 2016;11(4):e0153306.
12. Pham PH, Lumsden JS, Tafalla C, Dixon B, Bols NC. Differential effects of viral hemorrhagic septicaemia virus (VHSV) genotypes IVa and IVb on gill epithelial and spleen macrophage cell lines from rainbow trout (Oncorhynchus mykiss). Fish Shellfish Immunol. 2013;34(2):632–40.
13. Castro R, Abós B, Pignatelli J, Von Gersdorff JL, Granja AG, Buchmann K, Tafalla C. Early immune responses in rainbow trout liver upon viral hemorrhagic septicemia virus (VHSV) infection. PLoS ONE. 2014;9(10):e111084.
14. Qian X, Ba Y, Zhuang Q, Zhong G. RNA-seq technology and its application in fish transcriptomics. OMICS. 2014;18(2):98–110.
15. Palstra AP, Beltran S, Burgerhout E, Brittijn SA, Magnoni LJ, Henkel CV, Jansen HJ, Thillart GE, Spaink HP, Planas JV. Deep RNA Sequencing of the Skeletal Muscle Transcriptome in Swimming Fish. PLoS One. 2013;8(1):e53171.
16. Robinson NA, Robledo D, Sveen L, Daniels RR, Krasnov A, Coates A, Jin YH, Barrett LT, Lillehammer M, Kettunen AH, et al. Applying genetic technologies to combat infectious diseases in aquaculture. Rev Aquac. 2023;15(2):491–35.
17. Ali A, Rexroad CE, Thorgaard GH, Yao J, Salem M. Characterization of the rainbow trout spleen transcriptome and identification of immune-related genes. Front Genet. 2014;5:348.
18. Raida MK, Buchmann K. Innate immune response in rainbow trout (Oncorhynchus mykiss) against primary and secondary infections with Yersinia ruckeri O1. Dev Comp Immunol. 2009;33(1):35–45.
19. Thorgaard GH, Bailey GS, Williams D, Buhler DR, Kaattari SL, Ristow SS, Hansen JD, Winton JR, Bartholomew JL, Nagler JJ, et al. Status and opportunities for genomics research with rainbow trout. Comp Biochem Physiol B Biochem Mol Biol. 2002;133(4):609–46.
20. Ghaderzadeh M, Rahimi Mianji GH, Nejati Javaremi A, Shahbazian N. Effect of Viral Hemorrhagic Septicemia (VHS) disease on the biometric parameters in rainbow trout (Oncorhynchus mykiss). Vet Res Biol Prod. 2021;34(1):111–23.
21. Froese R. Cube law, condition factor and weight–length relationships: history, meta-analysis and recommendations. J Appl Ichthyol. 2006;22:241–53.
22. Peig J, Green AJ. New perspectives for estimating body condition from mass/length data: the scaled mass index as an alternative method. Oikos. 2009;118(12):1883–91.
23. Wilder SM, Raubenheimer D, Simpson SJ. Moving beyond body condition indices as an estimate of fitness in ecological and evolutionary studies. Funct Ecol. 2016;30(1):108–15.
24. Leal E, Fernández-Durán B, Guillot R, Ríos D, Cerdá-Reverter JM. Stress-induced effects on feeding behavior and growth performance of the sea bass (Dicentrarchus labrax): A self-feeding approach. J Comp Physiol B. 2011;181(8):1035–44.
25. Clancey E, Byers JA. The definition and measurement of individual condition in evolutionary studies. Ethology. 2014;120(9):845–54.
26. Timi JT, Poulin R. Why ignoring parasites in fish ecology is a mistake. Int J Parasitol. 2020;50(10-11):755–61.
27. Dorson M, Chevassus B, Torhy C. Comparative susceptibility of three species of char and of rainbow trout × char triploid hybrids to several pathogenic salmonid viruses. Dis Aquat Organ. 1991;11(3):217–24.
28. Quillet E, Dorson M, Le Guillou S, Benmansour A, Boudinot P. Wide range of susceptibility to rhabdoviruses in homozygous clones of rainbow trout. Fish Shellfish Immunol. 2007;22(5):510–9.
29. Snow M, Bain N, Black J, Taupin V, Cunningham CO, King JA, Skall HF, Raynard RS. Genetic population structure of marine viral haemorrhagic septicaemia virus (VHSV). Dis Aquat Organ. 2004;61(1-2):11–21.
30. Andrews S. A quality control tool for high throughput sequence data. 2010. http://www.bioinformatics.babraham.ac.uk/projects/fastqc/.
31. Bolger AM, Lohse M, Usadel B. Trimmomatic: a flexible trimmer for Illumina sequence data. Bioinformatics. 2014;30(15):2114–20.
32. Kim D, Pertea G, Trapnell C, Pimentel H, Kelley R, Salzberg SL. TopHat2 : accurate alignment of transcriptomes in the presence of insertions, deletions and gene fusions. Genome Biol. 2013;14:R36.
33. Langmead B, Salzberg S. Fast gapped-read alignment with Bowtie 2. Nat Methods. 2012;9:357–59 .
34. Berthelot C, Brunet F, Chalopin D, Juanchich A, Bernard M, Noël B, et al. The rainbow trout genome provides novel insights into evolution after whole-genome duplication in vertebrates. Nat Commun. 2014;5:3657.

35. Trapnell C, Roberts A, Goff L, Pertea G, Kim D, Kelley DR, Pimentel H, Salzberg SL, Rinn JL, Pachter L. Differential gene and transcript expression analysis of RNA-seq experiments with TopHat and Cufflinks. Nat Protoc. 2012;7:562–78.
36. Goff LA, Trapnell C, Kelley D. CummeRbund: visualization and exploration of Cufflinks high-throughput sequencing data. (R package version 2.48.0, 2024). https://www.bioconductor.org/packages/release/bioc/html/cummeRbund.html.
37. Kanehisa M, Goto S. KEGG: Kyoto Encyclopedia of Genes and Genomes. Nucleic Acids Res. 2000;28(1):27–30.
38. Huang DW, Sherman BT, Tan Q, Collins JR, Alvord WG, Roayaei J, Stephens R, Baseler MW, Lane HC, Lempicki RA. The DAVID Gene Functional Classification Tool: a novel biological module-centric algorithm to functionally analyze large gene lists. Genome Biol. 2007;8(9):R183.
39. Warde-Farley D, Donaldson SL, Comes O, Zuberi K, Badrawi R, Chao P, Franz M, Grouios C, Kazi F, Lopes CT, et al. The GeneMANIA prediction server: biological network integration for gene prioritization and predicting gene function. Nucleic Acids Res. 2010;38:214–20.
40. Rychlik W. OLIGO 7 primer analysis software. Methods Mol Biol. 2007;402:35–60.
41. Duesund H, Nylund S, Watanabe K, Ottem KF, Nylund A. Characterization of a VHS virus genotype III isolated from rainbow trout (Oncorhychus mykiss) at a marine site on the west coast of Norway. Virol J. 2010;7:19.
42. Pfaffl MW. A new mathematical model for relative quantification in real-time RT-PCR. Nucleic Acids Res. 2001;29(9):e45.
43. Ruijter JM, Barnewall RJ, Marsh IB, Szentirmay AN, Quinn JC, van Houdt R, Gunst QD, van den Hoff MJB. Efficiency Correction Is Required for Accurate Quantitative PCR Analysis and Reporting. Clin Chem. 2021;67(6):829–42.
44. Schroeder A, Mueller O, Stocker S, Salowsky R, Leiber M, Gassmann M, Lightfoot S, Menzel W, Granzow M, Ragg T. The RIN: an RNA integrity number for assigning integrity values to RNA measurements. BMC Molecular Biol. 2006;7:3.
45. Haghighi Khiabanian Asl A, Bandehpour M, Sharifnia Z, Kazemi B. Diagnosis of viral haemorrhagic septicaemia (VHS) in Iranian rainbow trout aquaculture by pathology and molecular techniques. Bull Eur Ass Fish Pathol. 2008;28(5):170.
46. Ahmadivand S, Soltani M, Mardani K, Shokrpoor S, Rahmati-Holasoo H, Mokhtari A, Hasanzadeh R. Isolation and identification of viral hemorrhagic septicemia virus (VHSV) from farmed rainbow trout (Oncorhynchus mykiss) in Iran. Acta Trop. 2016;156:30–6.
47. Fattahi F, Akhlaghi M, Mohammadi A, Soltanian S, Shahbazian N. Phylogenetic analysis of viral hemorrhagic septicemia virus from recent outbreaks in some of the farmed rainbow trout, Oncorhynchus mykiss (Walbaum, 1792). Iran J Fish Sci. 2020;19(3):1384–95.
48. Ahmadivand S, Palić D, Weidmann M. Molecular Epidemiology of Novirhabdoviruses Emerging in Iranian Trout Farms. Viruses. 2021;13(3):448.
49. McLauchlan PE, Collet B, Ingerslev E, Secombes CJ, Lorenzen N, Ellis AE. DNA vaccination against viral haemorrhagic septicaemia (VHS) in rainbow trout: size, dose, route of injection and duration of protection-early protection correlates with Mx expression. Fish Shellfish Immunol. 2003;15(1):39–50.
50. Ortega-Villaizan MDM, Chico V, Perez L. Fish Innate Immune Response to Viral Infection-An Overview of Five Major Antiviral Genes. Viruses. 2022;14(7):1546.
51. Robertsen B. Expression of interferon and interferon-induced genes in salmonids in response to virus infection, interferon-inducing compounds and vaccination. Fish Shellfish Immunol. 2008;25(4):351–7.
52. Munang'andu HM, Mutoloki S, Evensen Ø. Acquired immunity and vaccination against infectious pancreatic necrosis virus of salmon. Dev Comp Immunol. 2014;43(2):184–96.
53. Levraud JP, Jouneau L, Briolat V, Laghi V, Boudinot P. IFN-Stimulated Genes in Zebrafish and Humans Define an Ancient Arsenal of Antiviral Immunity. J Immunol. 2019;203(12):3361–73.
54. Petes C, Odoardi N, Gee K. The Toll for Trafficking: Toll-Like Receptor 7 Delivery to the Endosome. Front. Immunol. 2017;8:1075.
55. Takeda K, Kaisho T, Akira S. Toll-like receptors. Annu Rev Immunol. 2003;21:335–76.
56. Akira S, Uematsu S, Takeuchi O. Pathogen recognition and innate immunity. Cell. 2006;124(4):783–801.
57. Beutler BA. TLRs and innate immunity. Blood. 2009;113(7):1399–407.
58. Foster SL, Hargreaves DC, Medzhitov R. Gene-specific control of inflammation by TLR-induced chromatin modifications. Nature. 2007;447(7147):972–8.
59. Zhang YB, Gui JF. Molecular regulation of interferon antiviral response in fish. Dev Comp Immunol. 2012;38(2):193–202.
60. Collet B, Secombes CJ. Type I-interferon signalling in fish. Fish Shellfish Immunol. 2002;12(5):389–97.
61. Hegedus Z, Zakrzewska A, Agoston VC, Ordas A, Rácz P, Mink M, Spaink HP, Meijer AH. Deep sequencing of the zebrafish transcriptome response to mycobacterium infection. Mol Immunol. 2009;46(15):2918–30.
62. Stafford JL, Ellestad KK, Magor KE, Belosevic M, Magor BG. A toll-like receptor (TLR) gene that is up-regulated in activated goldfish macrophages. Dev Comp Immunol. 2003;27(8):685–98.
63. Wang W, Shen Y, Pandit NP, Li J. Molecular cloning, characterization and immunological response analysis of Toll-like receptor 21 (TLR21) gene in grass carp, Ctenopharyngodon idella. Dev Comp Immunol. 2013;40(3-4):227–31.
64. Meijer AH, Gabby Krens SF, Medina Rodriguez IA, He S, Bitter W, Ewa Snaar-Jagalska B, Spaink HP. Expression analysis of the Toll-like receptor and TIR domain adaptor families of zebrafish. Mol Immunol. 2004;40(11):773–83.
65. Zhao F, Li YW, Pan HJ, Shi CB, Luo XC, Li AX, Wu SQ. Expression profiles of toll-like receptors in channel catfish (Ictalurus punctatus) after infection with Ichthyophthirius multifiliis. Fish Shellfish Immunol. 2013;35(3):993–7.
66. Pridgeon JW, Shoemaker CA, Klesius PH. Identification and expression profile of multiple genes in the anterior kidney of channel catfish induced by modified live Edwardsiella ictaluri vaccination. Vet Immunol Immunopathol. 2010;134(3-4):184–98.
67. Brownlie R, Zhu J, Allan B, Mutwiri GK, Babiuk LA, Potter A, Griebel P. Chicken TLR21 acts as a functional homologue to mammalian TLR9 in the recognition of CpG oligodeoxynucleotides. Mol Immunol. 2009;46(15):3163–70.
68. Lee CC, Avalos AM, Ploegh HL. Accessory molecules for Toll-like receptors and their function. Nat Rev Immunol. 2012;12(3):168–79.
69. Quiniou SM, Boudinot P, Bengtén E. Comprehensive survey and genomic characterization of Toll-like receptors (TLRs) in channel catfish, Ictalurus punctatus: identification of novel fish TLRs. Immunogenetics. 2013;65(7):511–30.
70. Lutfalla G, Roest Crollius H, Stange-Thomann N, Jaillon O, Mogensen K, Monneron D. Comparative genomic analysis reveals independent expansion of a lineage-specific gene family in vertebrates: the class II cytokine receptors and their ligands in mammals and fish. BMC Genomics. 2003;4(1):29.
71. Zou J, Clark MS, Secombes CJ. Characterisation, expression and promoter analysis of an interleukin 10 homologue in the puffer fish, Fugu rubripes. Immunogenetics. 2003;55(5):325–35.
72. Grayfer L, Hodgkinson JW, Hitchen SJ, Belosevic M. Characterization and functional analysis of goldfish (Carassius auratus L.) interleukin-10. Mol Immunol. 2011;48(4):563–71.
73. Piazzon MC, Savelkoul HS, Pietretti D, Wiegertjes GF, Forlenza M. Carp Il10 Has Anti-Inflammatory Activities on Phagocytes, Promotes Proliferation of Memory T Cells, and Regulates B Cell Differentiation and Antibody Secretion. J Immunol. 2015;194(1):187–99.
74. Zou J, Carrington A, Collet B, Dijkstra JM, Yoshiura Y, Bols N, Secombes C. Identification and bioactivities of IFN-gamma in rainbow trout Oncorhynchus mykiss: the first Th1-type cytokine characterized functionally in fish. J Immunol. 2005;175(4):2484–94.
75. Pijanowski L, Scheer M, Verburg-van Kemenade BM, Chadzinska M. Production of inflammatory mediators and extracellular traps by carp macrophages and neutrophils in response to lipopolysaccharide and/or interferon-γ2. Fish Shellfish Immunol. 2015;42(2):473–82.
76. Grayfer L, Garcia EG, Belosevic M. Comparison of macrophage antimicrobial responses induced by type II interferons of the goldfish (Carassius auratus L.). J Biol Chem. 2010;285:23537–47.

77. Yang K, Zhang S, Chen D, Zhang A, Wang X, Zhou H. IFN-γ-activated lymphocytes boost nitric oxide production in grass carp monocytes/macrophages. Fish Shellfish Immunol. 2013;35(5):1635–41.
78. Tsutsumi S, Mollapour M, Prodromou C, Lee CT, Panaretou B, Yoshida S, Mayer MP, Neckers LM. Charged linker sequence modulates eukaryotic heat shock protein 90 (Hsp90) chaperone activity. Proc Natl Acad Sci U S A. 2012;109(8):2937–42.
79. Mokhtar DM, Zaccone G, Alesci A, Kuciel M, Hussein MT, Sayed RKA. Main Components of Fish Immunity: An Overview of the Fish Immune System. Fishes. 2023;8(2):93.
80. Csermely P, Schnaider T, Soti C, Prohászka Z, Nardai G. The 90-kDa molecular chaperone family: structure, function, and clinical applications. A comprehensive review. Pharmacol Ther. 1998;79(2):129–68.
81. Eybalin M, Altschuler RA. Immunoelectron microscopic localization of neurotransmitters in the cochlea. J Electron Microsc Tech. 1990;15(3):209–24.
82. Jing R, Duncan CB, Duncan SA. A small-molecule screen reveals that HSP90β promotes the conversion of induced pluripotent stem cell-derived endoderm to a hepatic fate and regulates HNF4A turnover. Development. 2017;144(10):1764–74.
83. Nguyen M, Csermely P, Sőti C. Hsp90 chaperones PPARγ and regulates differentiation and survival of 3T3-L1 adipocytes. Cell Death Differ. 2013;20:1654–63.
84. Zou J, Secombes CJ. The Function of Fish Cytokines. Biology (Basel). 2016;5(2):23.
85. Persengiev SP, Zhu X, Dixit BL, Maston GA, Kittler EL, Green MR. TRF3, a TATA-box-binding protein-related factor, is vertebrate-specific and widely expressed. Proc Natl Acad Sci U S A. 2003;100(25):14887–91.
86. McIlwain DR, Berger T, Mak TW. Caspase functions in cell death and disease. Cold Spring Harb Perspect Biol. 2013;5(4):a008656.
87. Unsain N, Barker PA. New Views on the Misconstrued: Executioner Caspases and Their Diverse Non-apoptotic Roles. Neuron. 2015;88(3):461–74.
88. Hyman BT, Yuan J. Apoptotic and non-apoptotic roles of caspases in neuronal physiology and pathophysiology. Nat Rev Neurosci. 2012;13(6):395–406.
89. Kuranaga E. Caspase signaling in animal development. Dev Growth Differ. 2011;53(2):137–48.
90. Campisi L, Cummings RJ, Blander JM. Death-defining immune responses after apoptosis. Am J Transplant. 2014;14(7):1488–98.
91. Mukherjee, A., Williams, D. More alive than dead: non-apoptotic roles for caspases in neuronal development, plasticity and disease. Cell Death Differ. 2017;24:1411–21.
92. Fernando P, Brunette S, Megeney LA. Neural stem cell differentiation is dependent upon endogenous caspase 3 activity. FASEB J. 2005;19(12):1671–3.
93. Campbell DS, Holt CE. Apoptotic pathway and MAPKs differentially regulate chemotropic responses of retinal growth cones. Neuron. 2003;37(6):939–52.
94. Westphal D, Sytnyk V, Schachner M, Leshchyns'ka I. Clustering of the neural cell adhesion molecule (NCAM) at the neuronal cell surface induces caspase-8- and -3-dependent changes of the spectrin meshwork required for NCAM-mediated neurite outgrowth. J Biol Chem. 2010;285(53):42046–57.
95. Genet C, Verrier ER, Ciobotaru C, Klopp C, Esquerre D, Laloe D, Boudinot P, Quillet E. RNA-seq analysis of transcriptome response to VHS-V infection in two target tissues of resistant vs susceptible trout clonal lines. 10th World Congress of Genetics Applied to Livestock Production Proceedings. 2014.
96. Verrier ER, Dorson M, Mauger S, Torhy C, Ciobotaru C, Hervet C, Dechamp N, Genet C, Boudinot P, Quillet E. Resistance to a Rhabdovirus (VHSV) in Rainbow Trout: Identification of a Major QTL Related to Innate Mechanisms. PLoS ONE. 2013;8(2):e55302.
97. Verrier ER, Ehanno A, Biacchesi S, Le Guillou S, Dechamp N, Boudinot P, Bremont M, Quillet E. Lack of correlation between the resistances to two rhabdovirus infections in rainbow trout. Fish Shellfish Immunol. 2013;35(1):9–17.
98. Neiffer DL, Stamper MA. Fish sedation, analgesia, anesthesia, and euthanasia: considerations, methods, and types of drugs. ILAR J. 2009;50(4):343–60.
99. Sneddon LU, Clinical Anesthesia and Analgesia in Fish. J Exot Pet Med. 2012;21(1):32–43.
100. Guénette SA, Uhland FC, Hélie P, Beaudry F, Vachon P. Pharmacokinetics of eugenol in rainbow trout (Oncorhynchus mykiss). Aquaculture. 2007;266(1–4):262–5.
101. Leary S, Underwood W, Anthony R, Cartner S, Grandin T, Greenacre C, Gwaltney-Brant S, McCrackin MA, Meyer R, Miller D, et al. AVMA guidelines for the euthanasia of animals: 2020 edition. J Am Vet Med Assoc. 2020. p. 121. ISBN: 978-1-882691-09-8.
102. Ross LG, Ross B. Anaesthetic and sedative techniques for aquatic animals. 3rd ed. Wiley-Blackwell; 2008. p. 240. ISBN: 978-1-405-14938-9.

Publisher's Note